



**NTNU – Trondheim**  
Norwegian University of  
Science and Technology

# Ultrasound Based Localization and Quantification of Skeletal Muscle Contraction

**Max Heger**

Master of Science in Cybernetics and Robotics

Submission date: June 2014

Supervisor: Øyvind Stavdahl, ITK

Co-supervisor: Hans Torp, Sirkulasjon og bildediagnostikk

Norwegian University of Science and Technology  
Department of Engineering Cybernetics



## Abstract

Earlier experiments indicates that motor unit activity during isometric contractions can be imaged using a high-definition ultrasound scanner. In this study, ultrasound raw-data is analysed in MATLAB to localize and quantify the signal contributions from individual motor units during a muscle twitch. It is believed that imaging of mechanical response of contracting muscles can contribute to a more explicit study of muscle physiology and a more dexterous method for prosthetic control.

Two different experiments were executed during this study, one for determining the time delay between ECG electrode and ultrasound response and one for imaging muscle activity during an isometric contraction. Both test setups consisted of a GE-Vingmed Vivid E9 ultrasound scanner and an ML6-15 linear probe, where the scans were executed by using "Strain rate"-mode in the test option "Msc TVI" with a frequency of 15MHz, which resulted in frame rates between 120 and 220, depending on the depth of the scan.

To determine the time delay, an ECG electrode was connected to the probe and then submerged in a bucket filled with water and the last two ECG electrodes, where the time delay between the two responses were measured in MATLAB. To image muscle activity in a sequence of ultrasound strain rate images, the probe were placed in a clamped and fixed position over the biceps, giving images perpendicular to muscle fibers. Scans of isometric muscle contractions were recorded, with ECG electrodes placed on each side of the probe to detect associated motor unit action potentials.

The measurements of the time delay between EMG and ultrasound response shows that there are an expected time delay between 6.68ms and 15.38ms, depending on the propagation velocity of the motor unit action potentials. This indicates that motor unit activity can be captured in ultrasound strain rate image sequences.

Motor unit behaviour in strain rate image sequences can be used for locating individual motor units, but this method struggles to identify overlapping motor units as individual. It was found that PCA for feature extraction in combination with a cluster based classification algorithm would be a more robust and time-saving method for localization of individual motor units.



## Sammendrag

Tidligere eksperimenter indikerer at motoriske enheters aktivitet under isometriske kontraksjoner kan bli avbildet ved bruk av en høyoppløselig ultralydskanner. I dette studiet er ultralyd rådata analysert i MATLAB for å lokalisere og kvantifisere bidragene fra individuelle motoriske enheter under en kontraksjon. Hvis den mekaniske responsen fra muskler under en sammentrekning kan bli avbildet, kan dette bidra til en mer eksplisitt studie av muskelfysiologi og være en mulig metode for protesestyring.

To ulike eksperimenter ble utført i dette studiet, en for å bestemme tidsforsinkelsen mellom EKG elektroder og ultralyd respons og en for å avbilde muskelaktivitet under en isometrisk bevegelse. Begge testoppsettene bestod av en GE-Vingmed Vivid E9 ultralydskanner og en ML6-15 lineær probe, hvor opptakene ble utført ved å bruke "Strain rate"-mode i testopsjonen "Msc TVI" med en frekvens på 15MHz, som resulterte i bildefrekvenser mellom 120 og 220, avhengig av dybden valgt under opptak.

For å bestemme tidsforsinkelsen, ble en EKG-elektrode festet til proben og deretter nedsenket i en bøtte med vann og de to siste EKE-elektrodene, der tidsforsinkelsen mellom responsene ble målt i MATLAB. For å avbilde muskelaktivitet i en sekvens med ultralyd "strain rate" bilder, ble proben plassert i en fast posisjon over biceps, for å avbilde muskelen vertikalt på muskelfibrene. Opptak av isometriske muskelkontraksjoner ble tatt med EKG elektroder plassert på hver side av proben for å detektere motoriske enheters aksjonspotensial.

Målingene av tidsforskjellen mellom EMG og ultralyd respons viser at det er en forventet tidsforskjell mellom 6.68ms og 15.38ms, avhengig av propageringshastigheten til de motoriske enhetenes aksjonspotensial. Dette indikerer at individuelle motoriske enheters aktivitet kan sees i ultralyd "strain rate"-bildesekvenser.

Typisk oppførsel av motoriske enheter i en sekvens av ultralyd "strain rate"-bilder kan bli brukt til å lokalisere motoriske enheter, men denne metoden sliter med å indentifisere overlappende motoriske enheter som individuelle. En foreslått metode som benytter seg av prinsippal komponent analyse for å lokalisere individuelle motoriske enheter er presentert i dette studiet. Denne metoden i kombinasjon med en "klynge"-basert klassifiseringsalgoritme antas å være tidsbesparende og en mer robust metode for lokalising av motoriske enheter.



# *Acknowledgements*

During this project, I have received help from both NTNU and the Department of Circulation and Medical Imaging, NTNU. I would like to express my great appreciation to Øyvind Stavdahl for helping me along the way by supplying me with new and interesting literature and for feeding me with new ideas when I was stuck in the same mindset. I also wish to thank both Hans Torp and Lasse Løvstakken at St. Olavs Hospital for assistance with the ultrasound scanner and setting up a preferable test setup.

I would like to express my gratitude to Harald Martens, who introduced many different ways of utilizing principal component analysis, which now seems to be of use in a limitless amount of applications.

I would also like to offer my special thanks to Lars Lyse Moen for being a good confidant throughout the whole semester.





# Contents

<b>Abstract</b>	<b>i</b>
<b>Acknowledgements</b>	<b>v</b>
<b>Contents</b>	<b>vi</b>
<b>List of Figures</b>	<b>xi</b>
<b>List of Tables</b>	<b>xiii</b>
<b>Abbreviations</b>	<b>xv</b>
<b>Symbols</b>	<b>xvii</b>
<b>1 Introduction</b>	<b>1</b>
1.1 History . . . . .	1
1.2 Motivation . . . . .	4
1.3 Objective and interpretation of the assignment . . . . .	4
1.4 Outline . . . . .	6
<b>2 Theory</b>	<b>9</b>
2.1 Skeletal muscles . . . . .	9
2.1.1 Motor units . . . . .	11
2.2 Electromyography (EMG) . . . . .	13
2.3 Ultrasound instrumentation . . . . .	13
2.3.1 Basic Instrumentation . . . . .	14
2.3.2 Imaging modes . . . . .	16
2.3.3 Doppler effect . . . . .	17
2.3.4 Phase analysis . . . . .	18
2.3.5 Strain and strain rate . . . . .	19
2.3.6 Motor unit behaviour in ultrasound strain rate images . . . . .	20
2.3.7 Time delay between ECG electrodes and ultrasound response . . . . .	21
2.4 Cross correlation . . . . .	22
2.5 Data reduction and classification methods . . . . .	22
2.5.1 Cluster analysis (CA) and factor analysis (FA) . . . . .	22
2.5.2 Single value decomposition (SVD) . . . . .	24

---

2.5.3	Principal component analysis (PCA)	25
2.5.4	Partial least squares regression (PLSR)	28
2.5.5	Linear discriminant analysis (LDA)	29
2.5.6	k-nearest neighbours (kNN)	29
2.5.7	Support vector machine (SVM)	31
2.6	Feature extraction using SVD	32
<b>3</b>	<b>Methods and implementation</b>	<b>39</b>
3.1	Loading ultrasound raw-data in MATLAB	39
3.2	Equipment and test setup	41
3.3	Time delay between ECG electrodes and ultrasound response	42
3.3.1	Test setup and experiment execution	42
3.3.2	Problems	44
3.3.3	Program for calculating time delay	44
3.4	Program for motor unit localization	46
3.4.1	Synchronization of EMG and ultrasound sequence, align_US_ECG	46
3.4.2	Get and filter strain rate data, get_and_filter_SR_data	47
3.4.3	Data representation and response to contraction, make_isosurf_obj	49
3.4.4	Localization of regions of contraction, make_and_plot_projections	52
3.5	Data reduction as a method for localization, feature_extraction	53
3.5.1	Data reduction method	53
3.5.2	Program for feature extraction using SVD, feature_extraction	53
<b>4</b>	<b>Results and analysis</b>	<b>55</b>
4.1	Time delay between EMG and ultrasound response	55
4.2	Strain rate	57
4.3	Localization based on motor unit behaviour	59
4.3.1	Motor unit behaviour	59
4.3.2	Localization	61
4.4	Feature extraction using SVD for localization of motor units	62
4.4.1	Ultrasound sequence containing one contraction	62
4.4.2	Ultrasound sequence containing multiple contractions	68
<b>5</b>	<b>Discussion</b>	<b>75</b>
5.1	Time delay between EMG and ultrasound response	75
5.2	Motor Unit Localization	76
<b>6</b>	<b>Conclusion</b>	<b>79</b>

---

<b>7</b>	<b>Future work</b>	<b>81</b>
7.1	Data acquisition . . . . .	81
7.2	Automatic localization . . . . .	81
7.3	Mapping of motor units . . . . .	82
7.4	Prosthetics . . . . .	82
<b>A</b>	<b>Project description</b>	<b>83</b>
<b>B</b>	<b>Sequences of strain rate images</b>	<b>87</b>
<b>C</b>	<b>Abstract for IEEE article</b>	<b>91</b>
C.1	Ultrasound Strain Rate Imaging of Individual Muscle Motor Units . . . . .	91
<b>D</b>	<b>DVD overview</b>	<b>93</b>
<b>E</b>	<b>Figure references</b>	<b>95</b>



# List of Figures

2.1	Skeletal muscle anatomy . . . . .	10
2.2	Motor unit territory (MUT) . . . . .	11
2.3	MUAP propagation in muscle fibers . . . . .	12
2.4	ECG sequence containing two contractions . . . . .	12
2.5	Transmitting and receiving side of an ultrasound scanner . . . . .	14
2.6	B-mode image of the anterior compartment of the upper arm . . . . .	15
2.7	Illustration of the Doppler effect . . . . .	17
2.8	Illustration of phase shift . . . . .	18
2.9	PDF of Gaussian distribution as an analogy for MU behaviour. . . . .	21
2.10	Illustration of cluster analysis . . . . .	23
2.11	Conversion from 3D strain rate sequence to 2D data matrix . . . . .	27
2.12	Illustration of the SVD algorithm . . . . .	28
2.13	Illustration of the kNN algorithm . . . . .	29
2.14	Illustration of the SVM algorithm . . . . .	31
2.15	Four different Gaussian distributions used to represent MUs . . . . .	32
2.16	Images showing the location of the four motor units. . . . .	33
2.17	Energy function . . . . .	34
2.18	SR images of the four leading PCs . . . . .	35
3.1	Class diagram for the mUDT program . . . . .	40
3.2	Test set-up for measuring time delay between ECG and ultrasound . . . . .	43
3.3	ECG response when submerging electrode in water, with a vertical blue line showing when the ECG electrode reacts to the water. . . . .	43
3.4	Ultrasound response when sinking probe in water, with a vertical blue line showing when the probe reacts to the water. . . . .	43
3.5	Flow chart for time delay calculation program . . . . .	44
3.6	Localization_auto program layout . . . . .	46
3.7	get_and_filter_SR_data program layout . . . . .	47
3.8	Weighted spatial filter . . . . .	48
3.9	make_isosurf_obj program layout . . . . .	49
3.10	EMG data for locating start time of contractions . . . . .	51
3.11	make_and_plot_projections program layout . . . . .	52
3.12	Communication diagram for the classification program . . . . .	53
4.1	Statistical data for time delay between ECG and ultrasound response . . . . .	56
4.2	Localization of motor units . . . . .	58

---

4.3	Strain rate image with ECG to shown time frame . . . . .	59
4.4	Six strain rate images showing different frames during a contraction	60
4.5	EMG response with marked time steps . . . . .	60
4.6	Isosurface images . . . . .	61
4.7	All strain rate images during a contraction added together . . . . .	62
4.8	Energy function . . . . .	63
4.9	Feature extracting using SVD, activity at time steps . . . . .	63
4.10	Feature extracting using SVD, pixels . . . . .	64
4.11	Strain rate images of the three leading principal components . . . . .	65
4.12	Feature extracting using SVD, activity at time steps . . . . .	66
4.13	Feature extraction using SVD, pixels . . . . .	67
4.14	ECG sequence containing four contractions . . . . .	68
4.15	Strain rate images of the four contractions in figure 4.14 . . . . .	69
4.16	Isosurface plot of strain rate data with chosen regions of contraction marked . . . . .	69
4.17	Strain rate images of the three leading principal components . . . . .	70
4.18	Feature extracting using SVD, pixels . . . . .	71
4.19	Feature extracting using SVD, showing score per time . . . . .	72
5.1	Figure showing an example of the Q-analysis window marked with a time delay of approximately 15 ms . . . . .	76
B.1	EMG and SR data showing different frames during contraction 1 . . .	87
B.2	EMG and SR data showing different frames during contraction 2 . . .	88
B.3	EMG and SR data showing different frames during contraction 3 . . .	89
B.4	EMG and SR data showing different frames during contraction 4 . . .	90
C.1	Image of the Q-analysis tool showing one contraction . . . . .	92

# List of Tables

3.1	Test equipment . . . . .	41
3.2	Expected time delays . . . . .	42
4.1	Mean delays and standard deviation . . . . .	55





# Abbreviations

<b>AP</b>	<b>Action Potential</b>
<b>BB</b>	<b>Biceps Brachii</b>
<b>B-mode</b>	<b>Brightness-mode</b>
<b>Br</b>	<b>Brachialis</b>
<b>CA</b>	<b>Cluster Analysis</b>
<b>CDI</b>	<b>Colour Doppler Imaging</b>
<b>CPCA</b>	<b>Classical Principal Component Analysis</b>
<b>DoF</b>	<b>Degrees of Freedom</b>
<b>ECG</b>	<b>ElectroCardioGraphy</b>
<b>EMG</b>	<b>ElectroMyoGraphy</b>
<b>EUD</b>	<b>Electro-Ultrasonic Delay</b>
<b>FA</b>	<b>Factor Analysis</b>
<b>FR</b>	<b>Frame Rate</b>
<b>FOV</b>	<b>Field Of View</b>
<b>FT</b>	<b>Frame Time</b>
<b>IQ</b>	<b>In-phase Quadrature</b>
<b>kNN</b>	<b>k-Nearest Neighbour</b>
<b>LDA</b>	<b>Linear Discriminant Analysis</b>

---

<b>MES</b>	<b>MyoElectric Signal</b>
<b>MMD</b>	<b>Measured Mean Delay</b>
<b>M-mode</b>	<b>Motion-mode</b>
<b>MRI</b>	<b>Magnetic Resonance Imaging</b>
<b>MU</b>	<b>Motor Unit</b>
<b>MUAP</b>	<b>Motor Unit Action Potential</b>
<b>MUT</b>	<b>Motor Unit Territory</b>
<b>PC</b>	<b>Principal Component</b>
<b>PCA</b>	<b>Principal Component Analysis</b>
<b>PDF</b>	<b>Probability Density Function</b>
<b>PLSR</b>	<b>Partial Least Squares Regression</b>
<b>PRF</b>	<b>Pulse Repetition Frequency</b>
<b>PSD</b>	<b>Power Spectral Density</b>
<b>Q-analysis</b>	<b>Quantitative analysis</b>
<b>RF</b>	<b>Radio Frequency</b>
<b>sEMG</b>	<b>surface ElectroMyoGraphy</b>
<b>SMG</b>	<b>SonoMyoGraphy</b>
<b>SR</b>	<b>Strain Rate</b>
<b>SRI</b>	<b>Strain Rate Imaging</b>
<b>STD</b>	<b>STandard Deviation</b>
<b>SVD</b>	<b>Single Value Decomposition</b>
<b>SVM</b>	<b>Support Vector Machine</b>
<b>TVI</b>	<b>Tissue Velocity Imaging</b>

# Symbols

$c$	speed of sound	$\frac{m}{s}$
$\lambda$	wave length	m
$f_d$	doppler frequency	Hz
$f$	frequency of transmitted wave	Hz
$v$	tissue velocity	$\frac{m}{s}$
$\Delta x$	strain length	m
$d$	distance	m
$t$	time	s
$PRF$	pulse repetition frequency	Hz
$\Delta\phi$	phase shift	rad
$VG = SR$	velocity gradient, strain rate	$\frac{1}{s}$
$\epsilon$	linear strain	



# Chapter 1

## Introduction

### 1.1 History

Skeletal muscles is what makes it possible for humans to move, communicate and interact with the environment. Knowledge of muscle function is therefore important when it comes to ergonomics, diagnosing and treating muscle disorders and controlling prostheses. There have not been much research on the use of ultrasound to measure muscle fiber activity during contractions, but the results from M. Heger (2013) [8], indicates that high-end ultrasound scanners can be used to localize geometric change in skeletal muscles on the scale of motor units (MUs) under an isometric contraction.

The use of ultrasound as a control method for prostheses is not in use today, but as ultrasound systems keeps getting smaller and better it may be possible to integrate ultrasound in the field of prosthetics. In P. W. Hodges et al. (2003) [21], ultrasound was used to estimate muscle activity by measuring fascicle lengths and muscle thickness in different muscles. It was found that ultrasound images can be used to detect low levels of muscle activity and provide a noninvasive method for detection of isometric muscle contractions, but not discriminate between moderate and strong contractions. This article is from 2003 and due to increased resolution in new ultrasound scanners it is believed that it now is possible to discriminate

between different levels of contractions. Sigrid Pillen (2010) [20] proved that small scale muscle twitches can be detected using ultrasound, which strengthens this hypothesis.

The possibility of using ultrasound to detect change of an active muscle has been attempted by Y. P. Zheng et al. (2005) [35] & (2010) [10] in both normal subjects and subjects missing a limb. In [35], the movement of forearm muscles during wrist movements were measured using ultrasound, a method they named sonomyography (SMG). The image sequence recorded were compared using image matching in form of 2D cross-correlation, and it was found that it is possible to detect morphological changes of forearm muscles by using Brightness-mode (B-mode) on a portable ultrasound system. Even though they did not find SMG feasible for prosthetic control, they encouraged further studies on the field, as scanners tends to get smaller with increased resolution and frame rate (FR).

Later studies by Y. P. Zheng et al. (2010) [10] & (2010) [34] showed that SMG performs better than electromyography (EMG) in tracking guided patterns and that these studies suggests that SMG control might be better than EMG control. It was also found that SMG had a huge advantage by providing more intuitive control, relieving the mental burden on the patient by easing the learning process of controlling the prosthesis.

Intramuscular EMG and surface EMG (sEMG) are two techniques that are currently used in the field of prosthetic control, but both methods have drawbacks and limitations. According to T. R. Farrell et al. (2005) [33], chronic intramuscular recordings for prosthetic use is not widely used, but it was found that insertion of electrodes in muscular tissue increased the accuracy of the EMG signal compared to sEMG. It was also found that fewer channels were needed for intramuscular EMG compared to sEMG, indicating that it is only necessary to gather data from a subset of muscles to maximize classification accuracy. Since this is an invasive method for control, it is less safe and may be a burden on the patient, which is not preferable.

Conventional non-invasive control system relies on the amplitude or acceleration of EMG signals, but due to cross talk and differentiation between joint motions, sEMG has limited specificity for deep muscles [26]. To overcome the limitations of sEMG, sophisticated pattern recognition strategies have been applied, although these strategies does not produce robust proportional signal for fine control. Even though some invasive techniques are fairly good, there continuous to be a need for a non-invasive robust sensing strategy to improve upon myoelectric systems.

In Siddharta et al. (2014) [26] a system consisting of a wearable mechanically scanned 7.5 MHz single element ultrasound system were proposed to map muscle activity in the forearm. The experiments were executed on ten healthy volunteers by holding a probe fixed relative to the forearm using a cuff. The ultrasound B-mode images were then spatially filtered with a moving averaging operation and analysed using MATLAB. The activity pattern in the ultrasound images for different finger movements of each test subject were stored and correlated with known activity patterns and classified using the k nearest neighbour (kNN) method. Individual digit movements were associated with unique maps of activity, and found to be able to classify digit movements with 98 % accuracy.

The result from Siddharta et al. (2014) [26] shows that ultrasound can be used to classify single digit movement using a training set. In contrary to the experiments executed in [26], this study will not focus on classifying known movements, but individual MUs from a random isometric contraction, which the experiments done in [26] and M. Heger (2013) [8] indicates is possible. The studies done by Y. P. Zheng et al. [35], [10] and [34] also shows that SMG is able to detect change of a muscle in action, which is in accordance with S. Pillen [20] and P. W. Hodges [21]. This literature survey indicates that new high-end ultrasound scanners are able to image muscle activity on the scale of MUs. If this is possible, it is believed that MU activity can be localized and classified in a sequence of ultrasound images, containing one or multiple contractions.

## 1.2 Motivation

This project was initiated because it is believed that ultrasound as a method for prosthetic control have not reached its full potential. It is a fact that people in general want smaller, as well as more powerful electronic devices and the same applies for medical instruments such as ultrasound scanners. Unlike medical equipment like x-ray and magnetic resonance imaging (MRI), ultrasound has no known permanent negative effects on human tissue within the given mechanical index (MI) and thermal index (TI) limits, which makes it an interesting option when it comes to diagnostics and prosthetic control.

If individual MUs can be automatically localized when overlapping in time and space by the use of ultrasound, it is believed that ultrasound can be of use in the field of ergonomics and rehabilitation technology. If ultrasound can be used to detect MU activity in real time, ultrasound may improve prosthetic control by being more robust and increase the number of degrees of freedom (DoFs).

## 1.3 Objective and interpretation of the assignment

This study is a continuation of earlier work done in M. Heger (2013) [8]. In [8], all data were analysed using the quantitative analysis (Q-analysis) tool on a GE-Vingmed Vivid E9 ultrasound scanner. This study will explore the possibility of using ultrasound raw-data to localize and quantize signal contributions from individual MUs in recorded ultrasound sequences by using MATLAB. This study will make use of earlier collected data from [8]. The results from [8] have not properly accounted for the time delay between the electrocardiography (ECG) electrodes and ultrasound response, which must be examined before it can be concluded that individual MU activity has been imaged.



The project description for this assignment is stated in Appendix A and the assignments are divided into four parts. My interpretation of these tasks are stated in the list below.

1. To assure that MU activity has been captured in M. Heger [8], the time delay between ECG electrodes and ultrasound recordings has to be determined. The results found in [8] shows that there are a delay between the detection of contractions in the EMG signal and the response from the ultrasound scanner, so it is important to establish to what degree this delay impacts earlier interpretations of ultrasound data.
2. This task concerns the use of data reduction techniques as a potential method for decomposing sequences of ultrasound images to localize and quantify the signal contributions of individual MUs. Multiple MUs can be active during a contraction, so my interpretation of this task is to find the location and spread of all individual MUs during a small isometric contraction by the use of ultrasound strain rate images. This will be referred to as either localization of individual MUs or classification of MU activity in the rest of the report.
3. In [8], the ultrasound scanner was the only tool used for analysis. In this study, raw-data recordings from the ultrasound scanner has to be loaded in MATLAB for computation of strain rate (SR) and further analysis. Chosen method for localization also has to be implemented.
4. The optimal parameters and test setup for the given task will follow the optimal setup found in [8], which consisted of equipment and settings that optimized resolution and FR. If the gathered data from [8] is not sufficient, new ultrasound scans has to be executed to get satisfying data. Some data acquisition has to be done to measure the time difference between the ECG electrodes and ultrasound response, but this data will not be used for localization of individual MUs, as these scans are not executed on human tissue.

## 1.4 Outline

**Theory:** The theory chapter contains details about muscle anatomy and basic use of EMG and ultrasound, data reduction and classification methods. The content of this chapter is meant to cover needed background to understand the used methods and for interpretation of the results in this report. The subsection that contains information about different data reduction methods and classification methods are an overview of some existing methods and are not all used in this project, but it is a part of the project assignment. The chapters containing muscle anatomy, EMG and basic ultrasound instrumentation and imaging modes are taken from the theory chapter in M. Heger (2013) [8], but expressed a bit different. While the subsection about "feature extraction using SVD" is my own work.

**Methods and implementation:** Contains information on program functionality, how parameters are found and the chosen test setup for measuring the time delay between EMG and ultrasound response and measuring muscle activity. A detailed explanation containing important variables and function calls for the programs can be found in the comments in the programs located on the DVD. Except for the "mUDT"-program got from St. Olavs Hospital, all the programs and test setups are my own work.

Some of the collected data for determine the time delay were eliminated from the datasets because they did not show a typical response from the ultrasound or the ECG electrodes.

**Results:** The result chapter is split in four parts.

1. Results from the experiment concerning the time difference between EMG and ultrasound response.
2. Result of the strain rate (SR) calculations with a comparison to earlier experiments from [8].
3. Results from the programs for localizing individual MUs by looking for typical MU behaviour.

4. How the proposed method, "feature extraction using SVD", can be used for localization of MUs.

Number 2 is meant to show that the output from the programs are reasonable with respect to stated MU behaviour in the theory chapter, which have contributed to making a program for MU localization. The results from the MU behaviour based localization algorithm helped to verify that the proposed method in number 4 works. The raw-data used for localization of MUs are taken from the term project [8].

**Discussion:** The discussion is split in two parts, one concerning the time delay between EMG and ultrasound response and one concerning MU localization. A program for localizing MU activity by the use of the "feature extraction using SVD"-method has not been made during this study, but a proposed method is presented and discussed.

**Conclusion:** Summarises the conclusions that can be drawn from the results in this study.

**Future work:** Addresses possible future work based on the achieved results in this study.

**Appendix:** Contains five chapters:

- A Project description
- B Images showing SR images during four different contractions from the same sequence.
- C Contains the abstract submitted to and approved by the "IEEE International Ultrasonics Symposium", Chicago, Illinois USA. [http://ewh.ieee.org/conf/ius\\_2014/](http://ewh.ieee.org/conf/ius_2014/).
- D DVD overview. Description of where the different programs and ultrasound raw-data can be found.
- E Figure references. References to figures that are not self made.



# Chapter 2

## Theory

The main objective of this study is to localize signal contributions from individual MUs. To be able to understand gathered raw-data and get satisfying new data, it is fundamental to have basic knowledge about skeletal muscles, EMG and ultrasound. An introduction to basic ultrasound instrumentation, EMG and muscle anatomy are present in this chapter. For the purpose of locating individual MUs, an overview of data reduction methods and classification algorithms is also present in this chapter.

### 2.1 Skeletal muscles

The definition of a skeletal muscle is a muscle that is under voluntary control and connected to bones via tendons (Figure 2.1(a)). When a skeletal muscle is innervated by a somatic motor neuron, the muscle contracts and increases the tension on the tendons, making a joint move by pulling on the bones. Skeletal muscles contains a set of fascicles that contains numerous muscle fibers. Muscle fibers are covered by a plasma membrane called sarcolemma and consists of smaller subunits called myofibrils that consists of subunits called myofilaments. Myofibrils are divided axially by Z-discs and the region between two Z-discs is called a sarcomere, Figure 2.1(b). A sarcomere has a length between 1.5 and 3.5  $\mu m$ , depending on

the size of the muscle, and each muscle fiber consists of approximately 20 000 sarcomeres [7].

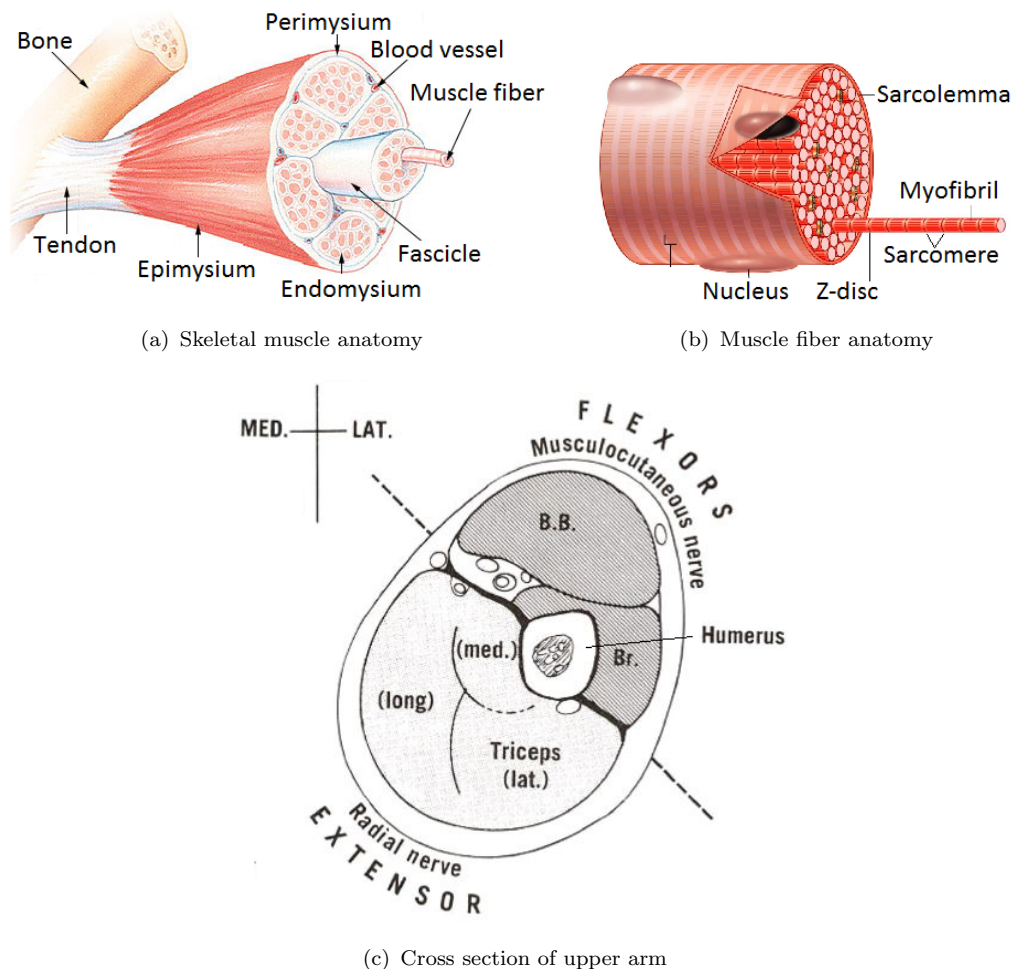


FIGURE 2.1: Skeletal muscle anatomy

When a muscle contracts, the Z-discs get pulled together resulting in a shortening of the sarcomeres, which is the source of the muscle contraction. The shortening of a sarcomere in axial direction also leads to an expansion in radial direction, making the muscle shorten in length and expand in circumference.

In M. Heger (2013) [8], the lateral muscles in the upper arm, Biceps Brachii (BB) and Brachialis (Br), shown in figure 2.1(c), were the targeted muscles. Since this study uses ultrasound data collected from [8], the lateral upper arm muscles are also the muscles of interest in this study.

### 2.1.1 Motor units

A motor unit (MU) is a somatic motor neuron together with all the muscle fibers it innervates. A somatic motor neuron can contain several axon terminals which are connected to different muscle fibers, through connection points called neuromuscular junctions. When a neurological signal, an action potential (AP), propagates along a somatic motor neuron, all the muscle fibers it is connected to will be innervated.

The recruitment of MUs follows the "size-principle": when utilizing greater force, active MUs are stimulated at a greater frequency before larger and larger MUs are activated. Larger MUs are usually located deeper in the muscles, which means that small contractions will innervate superficial MUs. Under a voluntary contraction, different MUs are stimulated fast and asynchronously.

Muscle fibers in BB varies in length and diameter, but according to P. E. Barkhaus et al. (2013) [19], they are approximately a few *cm* in length and 40-60  $\mu m$  in diameter. The muscle fibers in an MU does not necessarily lie next to each other, they are mostly spread out inside a region called the "motor unit territory" (MUT), which in the upper arm is estimated to be between 5 and 10 *mm* in diameter. Different MUs can be situated inside the same region, which means that MUTs can overlap, like in the illustration of MUTs in Figure 2.2.

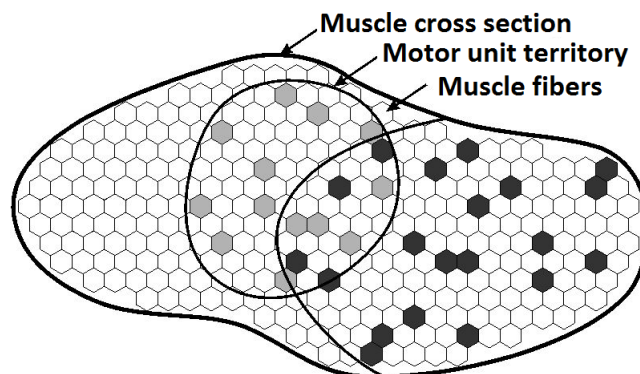


FIGURE 2.2: Motor unit territory (MUT)

When an AP arrives at the neuromuscular junction, the sarcolemma gets depolarized, causing the AP to propagate outwards and along the sarcolemma (Figure 2.3). Since a somatic motor neuron innervates a set of muscle fibers, the combined APs in all muscle fibers in an MU is called a motor unit action potential (MUAP), which is a signal that can be measured by EMG electrodes.

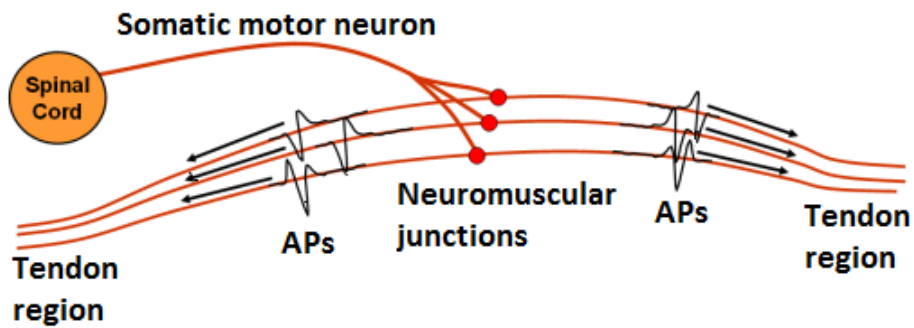


FIGURE 2.3: MUAP propagation in muscle fibers

Compared to AP propagation velocity (80-120 m/s [12]), the propagation velocity of MUAPs is slow. A typical MUAP last for 50 ms to 150 ms [8], depending on the size of the contraction, and has a propagation velocity of only 2-6m/s [7]. Figure 2.4 shows an recorded ECG sequence containing two typical EMG responses to contractions at  $Time = 0.1s$  and  $Time = 0.7s$ .

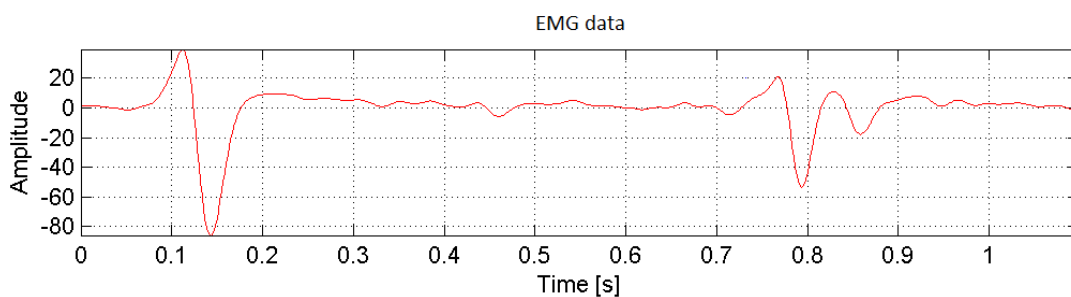


FIGURE 2.4: ECG sequence containing two contractions



## 2.2 Electromyography (EMG)

**EMG electrodes** detects the electrical potential of all MUs. This means that the detected signal is a combination of one or multiple MUAPs and since MUs are activated asynchronously, the detected contractions will vary in length. From the EMG signal, measurements of size, frequency and shape of MUAPs can be attained. The EMG signal is generally acquired by placing electrodes on the skin of the patient (sEMG) and the EMG signal is affected by skin condition, tissue condition, muscle strength, skeletal anatomy and range of motion.

In D. Farina et al. (2008) [5], MUAPs were compared with each other. It was found that MUAPs were considered indistinguishable and not uniquely in the sEMG when difference in mean energy was under 5%, and the number of MUAPs that could be identified depended on the number of used channels. Due to low-pass filtering effects of the tissues between active muscle fibers and the electrodes, MUAPs are often indistinguishable, but under some conditions, it is possible to identify MUAPs using sEMG.

**Controlling prostheses** by using sEMG electrodes are challenging and has certain limitations. A drawback for sEMG is the difficulty of differentiating between a wide specter of different MUAPs. The amplitude and frequency characteristics of the detected signal are most often not sufficient to distinguish between more than two different kinds of movement, which is a clear limitation of sEMG controlled prostheses, as the human hand has 22 DoFs [16].

**Using ultrasound** for controlling a prosthesis would have an advantage at this point. By detecting where the contraction originates, it may be possible to distinguish between more than two different classes of movement.

## 2.3 Ultrasound instrumentation

Ultrasound is deemed one of the safest diagnostic tools in the field of medicine and is used to diagnose patients in many different medical fields of study, especially

in cardiac and obstetrics. An ultrasound scanner has multiple settings and modes and the scanner is set up depending on what one want to examine. This sub chapter covers the basics of ultrasound instrumentation and how strain rate (SR) images are calculated in an ultrasound scanner.

### 2.3.1 Basic Instrumentation

The principle of ultrasound is the same as echo. By transmitting sound waves into tissue, it is possible to extract information based on the time and amplitude of received echo. The transducers in the tip of the ultrasound probe converts electrical energy to sound waves and vice versa, and the quality of the images are limited by the transducers performance.

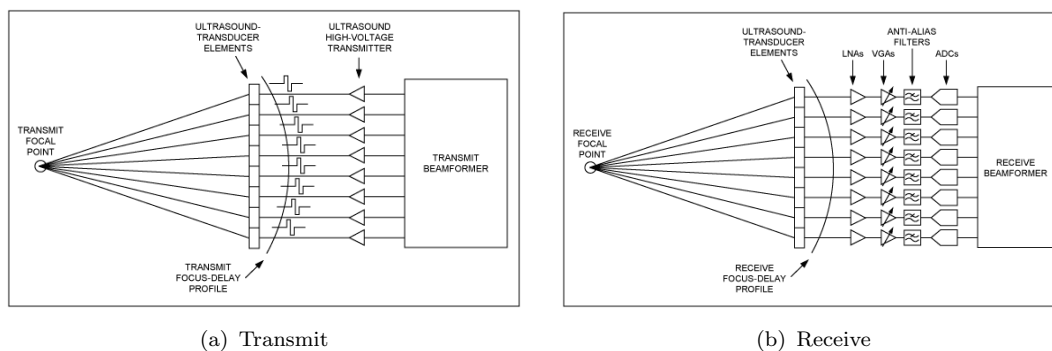


FIGURE 2.5: Transmitting and receiving side of an ultrasound scanner

The transmitters steer sound waves by activating different transducer elements with different time delays, as shown in Figure 2.5(a). The sound waves emitted from the active transducers are added in a desired focal point and the waves reflects off any object encountered along the path. Received echoes gets amplified, converted to digital signals and added together as shown in Figure 2.5(b). After all emitted sound waves have reflected off the focal point, the transducers emits a new array of sound waves to a new focal point along the same scan line.

The image acquired from an ultrasound scan shows a granular pattern, called speckle. Speckle is random, but still deterministic, and the size of the speckle

”particles” can be seen as the scanner resolution, which for high-end ultrasound scanners is up to  $0.1\text{mm}$  in display of muscle tissue [20]. Figure 2.6 shows a typical brightness-mode (B-mode) image of the anterior compartment in the upper arm, where BB, Br and the Humerus are marked.

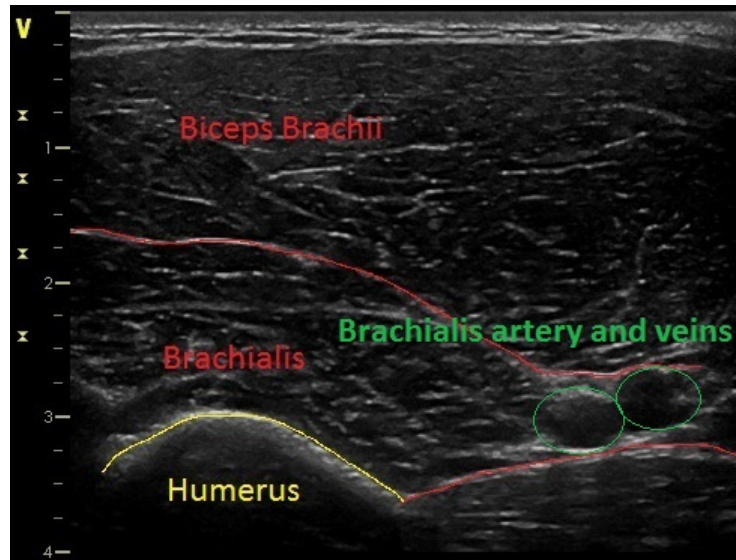


FIGURE 2.6: B-mode image of the anterior compartment of the upper arm

In this project, there are two parameters that are of utmost interest, frame rate (FR) and resolution. The resolution of the ultrasound system depends on the size of the aperture, frequency and the bandwidth of the transducer. Bigger aperture gives better resolution at the cost of FR, and the best achievable resolution is limited by the transducer bandwidth as this can not be altered. Higher frequency leads to better resolution and higher FR, but because tissue attenuation increases with frequency at a rate of  $1\frac{dB}{MHz*cm}$ , the depth of penetration is limited. This project will concentrate on superficial muscles in the upper arm, hence a high frequency is preferable.

The FR depends on number of scan lines and the pulse listen time (PLT), the maximum time it takes for the most distant echo to reach the transducer [2], which is dependent of the speed of sound in muscle tissue ( $c = 1560\frac{m}{s}$ ) and the depth of the scan. FR is the inverse of the frame time (FT) which depends on number of scan lines and the PLT, equation 2.3. For this project the FR should

be as high as possible without a significant reduction of resolution, so it may be preferable to decrease the aperture and number of scan lines to increase the FR at the cost of resolution.

$$PLT = \frac{2 * depth}{c} = 12.8 \frac{\mu s}{cm} * FOV \quad (2.1)$$

$$FT = PLT * n \quad (2.2)$$

$$FR = \frac{1}{FT} \quad (2.3)$$

**Ultrasound raw data** can be stored in different ways and the most common is to store the data as radio frequency (RF) or in-phase Quadrature (IQ) data. RF data denotes unprocessed data where the frequency information is intact. The IQ denotes the complex format, where a complex base-band modulation technique is applied to the RF data to reduce amount of data without losing essential information [13].

### 2.3.2 Imaging modes

This subsection only contains the imaging modes that has been used during this study.

- Brightness-mode (B-mode): The amplitude of received echoes determines the brightness of each point in the image.
- Motion mode (M-mode): Motion from a one-dimensional scan line is displayed on a vertical axis over time, and is used in conjunction with B-mode scanning, where active scan line can be chosen [17].
- Tissue velocity imaging (TVI): Whole image in color, showing tissue velocity.
- Strain rate imaging (SRI): Whole image in color for measuring deformation of tissue. This mode is often called colour Doppler imaging (CDI).

### 2.3.3 Doppler effect

The Doppler effect describes how the frequency of an emitted wave changes with the velocity of the emitter or observer. The principal of the Doppler effect is: if a source moves in the direction of the propagation of the waves, it is the frequency that increases, hence a decrease in wavelength, not the propagation velocity of the waves, see Figure 2.7. The Doppler effect requires a constant propagation velocity, which in the case of sound waves in muscle tissue is  $c = 1560 \frac{m}{s}$ . The propagation velocity is then given by the number of oscillations per seconds times the wavelength [29],

$$c = \lambda * f = 1560 \frac{m}{s}. \quad (2.4)$$

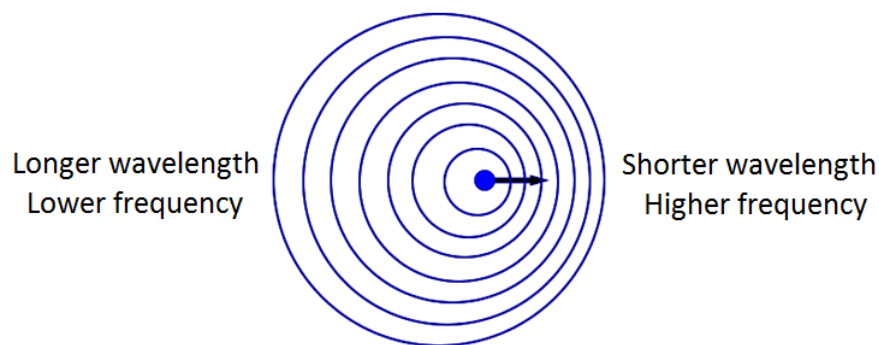


FIGURE 2.7: Illustration of the Doppler effect

**When ultrasound waves** are reflected from a moving structure, scatter, the wavelength and frequency of the returning waves are shifted. The difference in frequency, the Doppler frequency  $f_d$ , can be used to measure tissue velocity. In ultrasound, positive velocities are seen when an object moves towards the probe and negative when moving away.

In ultrasound, scatter moving relative to the source result in a Doppler effect that is twice as great, since the scatter initially is a moving observer that becomes a

moving source due to reflection. The Doppler equation in ultrasound is therefore given by [29]:

$$f_d = \frac{2 * f * v}{c} \quad (2.5)$$

### 2.3.4 Phase analysis

A sound wave can be seen as a sine wave, where every point along the wave can be described by the phase of the wave point. In CDI, the Doppler shift is calculated by the use of phase shift. To be able to analyse the Doppler shift in terms of phase shift between pulses, at least two pulses must be emitted rapidly. If two subsequent pulses are emitted, a different phase on the reflected signals will indicate that the scatterer has moved at a given velocity. The time between the pulses is given by the inverse of the pulse repetition frequency (PRF) and the travel distance of the scatterer is given by:

$$d = v * t = v * \frac{1}{PRF} \quad (2.6)$$

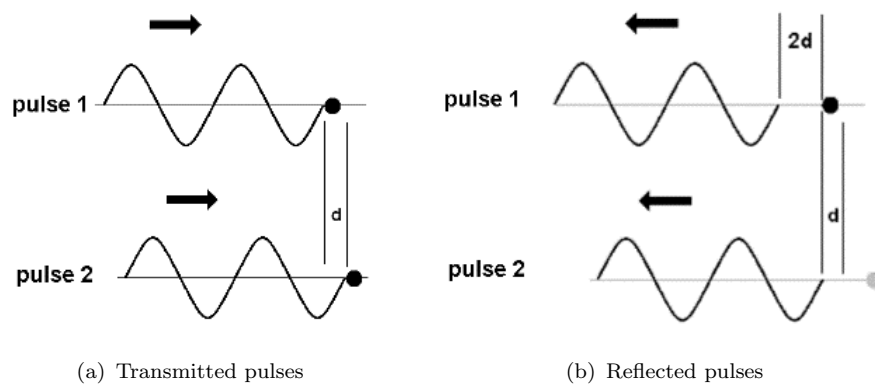


FIGURE 2.8: Illustration of phase shift

If the distance travelled by the scatterer between pulse 1 and 2 in Figure 2.8 is equal to  $d$ , pulse 2 has to travel a distance of  $2d$  longer than pulse 1. This means that the displacement of the waveform is  $2d$ , which corresponds to a phase shift of  $\Delta\phi$ .

This phase shift is calculated by finding the angle of the autocorrelation estimate with lag 1 ( $R1$ ) of the pulses, the shift that is needed for the pulse sequences to be as equal as possible [4].

If the distance  $2d$  in figure 2.8 is equal to the wavelength ( $\lambda$ ), this will result in a phase shift ( $\Delta\phi$ ) of  $2\pi$ . Equation 2.7 together with 2.4 and 2.6 results in Equation 2.11 for calculating the velocity [30].

$$\frac{2d}{\Delta\phi} = \frac{\lambda}{2\pi} \quad (2.7)$$

$$2d = \frac{c * \Delta\phi}{2\pi * f} \quad (2.8)$$

$$\frac{2 * v}{PRF} = \frac{c * \Delta\phi}{2\pi * f} \quad (2.9)$$

$$\Delta\phi = \angle R1 \quad (2.10)$$

$$v = \frac{c * PRF * \angle R1}{4\pi * f} \quad (2.11)$$

### 2.3.5 Strain and strain rate

Strain is a measurement of deformation of an object, relative to its original length. Strain is a dimensionless value that can be defined linearly by the Lagrangian formula 2.12 ([28]) that only describes strain in one dimension. Since SRI with linear probes only utilizes information in the axial direction, linear strain is sufficient for measuring strain in an ultrasound sequence from a linear probe.

$$\varepsilon = \frac{L - L0}{L0} = \frac{\Delta L}{L0} \quad (2.12)$$

Positive strain equals stretching, while negative strain is compression. The same goes for strain rate, instantaneous strain. In ultrasound instrumentation, strain rate is calculated from the velocity gradient.

As stated in Asbjørn Støylen [29], the velocity gradient was originally defined as the transmural velocity difference across the heart wall, divided by the instantaneous wall thickness, but this can be generalized to a definition in all directions:

$$VG = \frac{v_2 - v_1}{L} = \frac{\Delta v}{L} \quad (2.13)$$

SRI in ultrasound is done by utilizing tissue Doppler, using the longitudinal velocity gradient. SR is calculated by the velocity gradient of two arbitrary points over a segment with a fixed distance, the strain length  $\Delta x$ :

$$SR = \frac{v(x) - v(x + \Delta x)}{\Delta x} = VG \quad (2.14)$$

The difference between these two definition is that  $L$  in 2.13 changes, while  $\Delta x$  is constant. Equation 2.14 assumes that the strain is equally distributed over the length of the object, which results in an  $SR$  equal to  $VG$ . So Equation 2.14 is only an estimate of the strain rate [29].

### 2.3.6 Motor unit behaviour in ultrasound strain rate images

It is believed that different MUs will have variable size and unequal spatial distribution, but all MUs should behave equally. The SR images should show a gradually increasing SR with a gradually increasing region of expansion, before decreasing. An analogy for this response is the probability density function (PDF) of a Gaussian distribution, shown in Figure 2.9.

The SR is increasing as a response to a contraction and at the expectation value, time=5, the muscle fibers in the MU are fully expanded, and after this, the SR decreases.



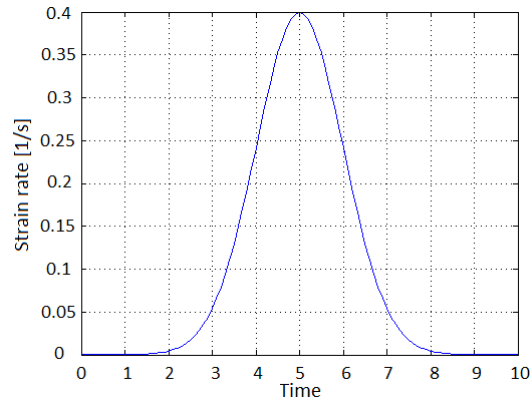


FIGURE 2.9: PDF of Gaussian distribution as an analogy for MU behaviour.

### 2.3.7 Time delay between ECG electrodes and ultrasound response

The results from M. Heger (2013) [8], indicates that it is possible to image muscular activity on the scale of MUs using a high-end ultrasound scanner. Before it can be concluded that MU activity has been imaged, the time difference between ECG electrodes and ultrasound response has to be taken into consideration.

The time delay between the ECG electrodes and ultrasound is supposed to be compensated for by the ultrasound system for the purpose of synchronising PQRST data with heart beats. Since the PQRST wave normally last for 0.4 to 1.5s, there can be a time delay negligible for heartbeat measuring that may not be negligible for measuring a faster response caused by an expansion of an MU.

In the project report [8], the electro-ultrasonic delay (EUD) was calculated to be between 4.3 and 13ms, depending on MUAP velocity. The EUD was measured visually from each ultrasound image and all the measurements were found to be inside the given boundaries (4.3 – 13ms).

## 2.4 Cross correlation

Cross correlation is a method for estimating the similarity of two waveforms and the cross correlation function can be defined discretely as:

$$(f * g)[n] = \sum_{m=-\infty}^{\infty} f^*[m]g[m + n], \quad (2.15)$$

where  $f$  and  $g$  are two waveforms,  $n$  is the lag and  $f^*$  is the complex conjugate of  $f$ . Cross correlation can be used to find where two waveforms are most similar. The peak of the cross correlation will indicate the number of steps needed to shift function  $g$  so that  $g$  and  $f$  overlaps the most. Cross correlation is widely used in the field of spectral analysis and computer vision and in this study, cross correlation is used to find phase angles for estimation of tissue velocity and to locate the arrival time of contractions in an EMG sequence.

## 2.5 Data reduction and classification methods

Data reduction is a process for minimizing the amount of data needed to increase storage efficiency and reduce execution time. A natural way to deal with high dimensional classification problems is to first reduce the dataset to a lower dimensional subspace before applying a classification strategy. In this study, data reduction and classification techniques will contribute to the classification process of MUs, localization of individual MU contributions.

### 2.5.1 Cluster analysis (CA) and factor analysis (FA)

**Cluster analysis (CA)** is a data reduction technique that tries to find natural groupings in data by grouping together objects with similar attributes [3]. In the case of an ultrasound sequence, each individual MU could be assigned to a group based on how deep the MU lies in the muscular tissue and the MUT. Since MUs

can overlap in time and space, this technique might not suffice for localization of individual MUs, unless it is possible to find MU attributes/characteristics that do not coincide.

Multiple attributes could be chosen, for example location and time of activation of MUs. Since different MUs gets activated asynchronously, it might be possible that the clusters could overlap and still locate different MUs based on temporal and spatial attributes. The result could look something like the example data in Figure 2.10.

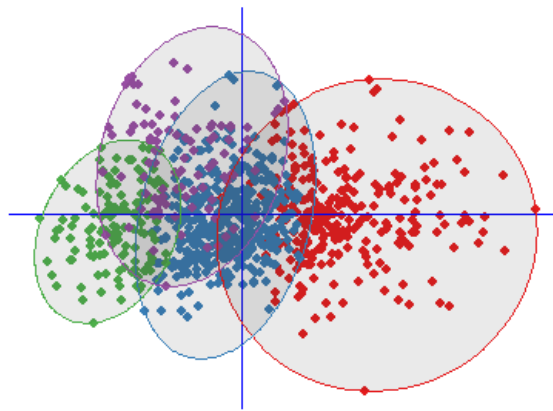


FIGURE 2.10: Illustration of cluster analysis

**Factor analysis (FA)** is a data reduction technique that tries to describe the covariance relationships among variables in terms of a few unobservable random quantities called factors [22]. The hypothesis when using FA is that there exists an underlying construct, a variable that has not been measured directly, where observed variables could be linear combinations of these underlying factors. If variables are correlated, FA can reduce the dataset to a smaller set of uncorrelated factors. These factors can then be used in place of the original variables, with the variation of the original data sustained [24].

PCA and FA are sometimes mistaken as the same statistical method, but there are differences. The biggest difference is that FA account for common variance in the data, while PCA results in PCs that account for a maximal amount of variance of observed variables [6].

Earlier results from M. Heger (2013) [8] indicates that captured MU activity in an ultrasound SR image basically is a cluster. Based on these results and Figure 2.10, it seems that CA would be good choice for classification of MUs.

## 2.5.2 Single value decomposition (SVD)

Single value decomposition (SVD) is a method for identifying and ordering the dimensions along which data points exhibit the most variation [1]. The basic idea behind SVD, is taking a high dimensional, highly variable set of data and reducing it to a lower dimensional space that exposes the substructure of the original data more clearly by ordering it from most variation to least [1].

SVD is based on a theorem which says that a rectangular matrix,  $X \in \mathbb{R}^{m \times n}$ , can be factorized into three matrices 2.16,

$$X = USV^T, \quad (2.16)$$

that have certain properties. If  $m > n$  and the rank of the data matrix  $X$  is  $r$ , these three matrices have the following properties [11]:

- $U$  is an  $m \times r$  column-orthonormal matrix. A matrix with orthogonal columns where each column is a unit vector.
- $S$  is a  $r \times r$  diagonal matrix, where the elements are the singular values (SVs) of the data matrix  $X$ .
- $V^T$  is an  $r \times n$  row-orthonormal matrix. A matrix with orthogonal rows where each row is a unit vector.

### 2.5.3 Principal component analysis (PCA)

**Principal component analysis (PCA)** is a classical data reduction technique for doing linear dimensionality reduction. PCA reduces the number of variables to a smaller number of principal components (PCs) which account for most of the variance of the observed variables. Classical PCA finds a small number,  $k$ , of linear combinations of the  $d$  input variables that capture most variability in the data, by looking for a  $k$ -dimensional linear subspaces that minimizes the sum of squared errors measured by the squared distances from the data points to the subspace [31]. PCA can be performed by different algorithms, but the most common is to perform PCA by taking the eigendecomposition, classical PCA (CPCA).

The CPCA algorithm is as follows [9]:

- 1:** Subtract data mean from each point, so that the data has zero mean.
- 2:** Scale each dimension by its variance, which ensures that found principal component directions is not influenced by the magnitude of the variable, meaning the units that that variable is measured in.
- 3:** Compute the covariance matrix of the data.
- 4:** Take the eigendecomposition of the covariance matrix:

$$\Sigma = VDVT^T, \quad (2.17)$$

where  $V$  contains the eigenvectors and the diagonal matrix  $D$  contains the eigenvalues, where the eigenvalues in  $D$  are sorted by size from highest to lowest. The first vector in  $V$  is called the first PC, the second is called the second PC and so on. PCs are uncorrelated and orthonormal and are a linear combination of weighted, observed variables.

- 5:** Compute the  $k$  largest eigenvectors of  $S$ .

PCA can perform poorly on the reduced data because PCA do not use the response variable and may therefore exclude components with little variance, but a great deal of information [31]. In the case of ultrasound strain rate images, places with small variance do not contain wanted information, so this is not a problem.

Because PCA computes eigenvalues and eigenvectors based on the covariance matrix, it is very sensitive to outlying points (noise). By filtering the data before taking the PCA, noise in the form of outlying points will be reduced and hopefully disappear completely.

PCA is wildly used in many field of studies, and in L. J. Hargrove et al. (2009) [15], PCA was used to improve classification accuracy in pattern-recognition-based myoelectric control. As stated in Chapter 2.2, myoelectric signals (MES) often contains contributions from more than one MU. In article [15], the measured MES were rotated by class-specific PC matrices to spatially decorrelate the measured data prior to feature extraction. It was shown that this processing technique significantly ( $p < 0.01$ ) reduced pattern recognition classification error for both intact limbed and transradial amputee subjects. This result indicates that PCA could be a good choice for pattern recognition in ultrasound images as well as for MES.

**PCA can be performed different ways.** Instead of taking the eigendecomposition (CPCA), it is possible to perform PCA by using SVD. If a data matrix,  $X$ , where each column is an image frame (Figure 2.11), the  $U$ ,  $S$  and  $V$  matrices will have the following interpretation [9]:

- $U$ : The columns of  $U$  will be orthogonal vectors, containing the principal component directions. These vectors will be equal to the eigenvectors of the covariance matrix.
- $S * V^T$ : The coefficients.

This gives the following representation for the data matrix  $X$ , where  $i$  represents a column and  $k$  the number of PCs:

$$X_i = S_{1,1}V_{1,i}U_1 + S_{2,2}V_{2,i}U_2 + \dots + S_{k,k}V_{k,i}U_k, \quad (2.18)$$

where each original image can be explained by some factor times the first PC, some factor times the second PC and so on.

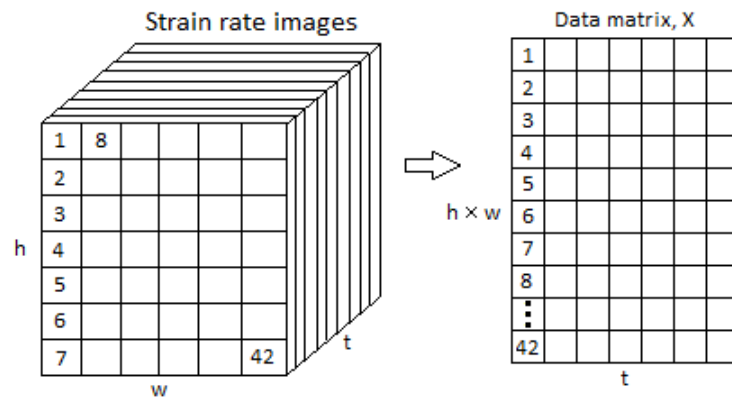


FIGURE 2.11: Conversion from 3D strain rate sequence to 2D data matrix

An example of performing PCA by using SVD is shown in figure 2.12, where SVD is performed on a two dimensional dataset containing 28 data points. It is seen that the first PC direction is the direction with the most variance, hence the largest eigenvector of the covariance matrix, while the second PC direction is the direction with least variation, the smallest eigenvector.

By using SVD for PCA, a decomposition containing three different matrices ( $U, S, V$ ) is achieved. The image in Figure 2.12 shows only the effect of the PCs in  $U$ , but by utilizing the coefficient  $SV^T$ , it is possible to extract information about the "importance" of the PCs. If all the points in Figure 2.12 was located on the first PC, the second PC would still be placed orthogonally on the first PC, but the coefficients would be zero, which means that the dataset is actually one dimensional.

Since SVD is a data reduction method, it is a question how many SVs that should be retained. A useful rule is to retain enough SVs to make up at least 90% of the "energy" in the S matrix, 90% of the sum of squares of all the singular values [11].

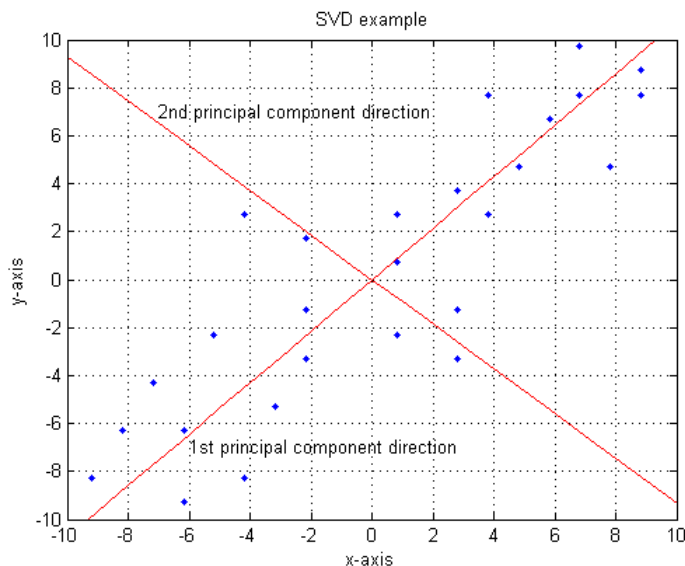


FIGURE 2.12: Illustration of the SVD algorithm

How SVD for PCA can be applied to localize individual MU contributions is found in Chapter 2.6.

### 2.5.4 Partial least squares regression (PLSR)

In Tim Wu et al. (2014) [32], multivariate partial least squares regression (PLSR) was used to determine the characteristics of a surrogate model of facial expressions. PLSR is a method for modelling relations between two sets of observed variables, the input parameters and the output responses [32]. In contrast to principal component regression (PCR), which uses PCA to compress the data into orthogonal components and use the data as regressors for the observed output responses, the PLSR creates the components by modelling the relationship between input and output, to ensure that the extracted components from the data are more relevant to the output. According to [32], PLSR achieves the same or better results as PCR, while using less and qualitatively different components. Even though PLSR may perform better than PCA, the interest lies in the variation of the ultrasound SR images, so it is believed that PCA by using SVD would be as good as PLSR for localizing individual MUs.



### 2.5.5 Linear discriminant analysis (LDA)

Linear discriminant analysis (LDA) is a commonly used technique for data classification and dimensionality reduction. In PCA, the shape and location of the original data set can change when transformed to a different space, whereas LDA does not change the location, but tries to provide more class separability [25]. LDA explicitly attempts to model differences between the classes of data, while PCA does not take the difference in class into account. LDA, PCA and FA all look for linear combinations of variables that explain the dataset, so these methods might be good choices for classifying MUs.

### 2.5.6 k-nearest neighbours (kNN)

The k-nearest neighbour algorithm is a non parametric technique, so it does not make any assumptions on the underlying data distribution. It is one of the simplest machine learning algorithms and can be used for both classification and regression. This method is a type of memory-based learning that compares new instances with instances earlier seen in training. Given a new instance, the algorithm calculates the distances to all the instances in the training set and picks the  $k$  closest instances [27]. An illustration of the algorithm for a two dimensional problem containing two groups, + and -, is shown in figure 2.13.

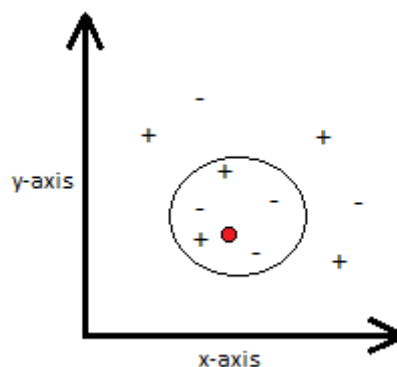


FIGURE 2.13: Illustration of the kNN algorithm

Depending on the  $k$ -value, the algorithm will give different answers to which class the red dot belongs to.

- $k = 1$ : outcome is a plus sign
- $k = 2$ : outcome is unknown
- $k = 3$ : outcome is a minus sign

This algorithm is easy to understand, but sensitive to noise and require large memory [14]. In the case of classification of individual MUs in SR images, kNN in combination with some algorithm for determine the distance to nearest neighbour could recognize new instances (pixels) as an already existing MU or be added to the training set. If the new instance can not be determined, it could mean that there are two overlapping MUs in this region and be classified to belong to both MUs. The kNN algorithm is a possible choice for classification of MUs, but CA, FA, LDA and PCA seems to be better choices for the task.

### 2.5.7 Support vector machine (SVM)

The support vector machine (SVM) algorithm requires a labelled training set to be of use. The output from the SVM algorithm is an optimal hyperplane, the hyperplane that gives the largest minimum distance to the different groups in the training set. Figure 2.14 shows where the optimal hyperplane would lay in a two dimensional data set containing two groups, circles and squares [18].

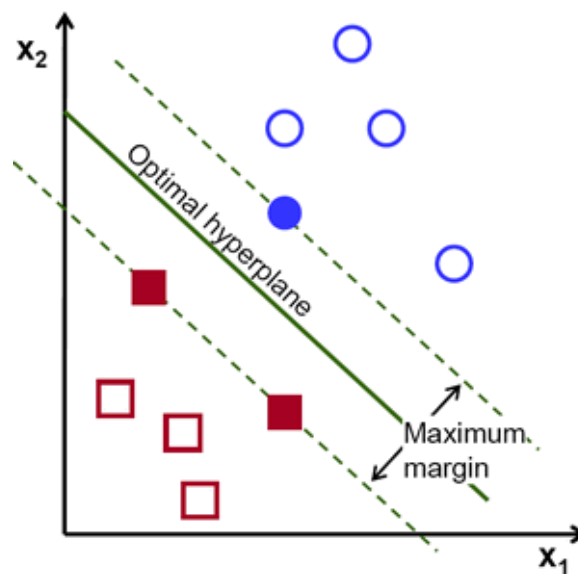


FIGURE 2.14: Illustration of the SVM algorithm

The classification is based on which side of the hyperplane the data point lays. A line is bad if it passes too close to the points, because it will be sensitive to noise, so the optimal line would be passing as far as possible from all points. In the case of classifying individual MUs, SVM would not be the preferred option compared to CA, FA, LDA or PCA, since individual MUs can overlap in space and therefore be difficult to classify by using this method.

## 2.6 Feature extraction using SVD

SVD is a data reduction method, which can also contribute to localization of individual MUs. To show this principal, a hypothetical SR ultrasound sequence has been made by representing MU activity by Gaussian distributions with equal variance and different expectation value, as seen in figure 2.15. As stated in Chapter 2.3.6, the expectation value indicates where the MU is fully contracted and since MU activation is asynchronous, the expectation values decides the sequence of MU activation.

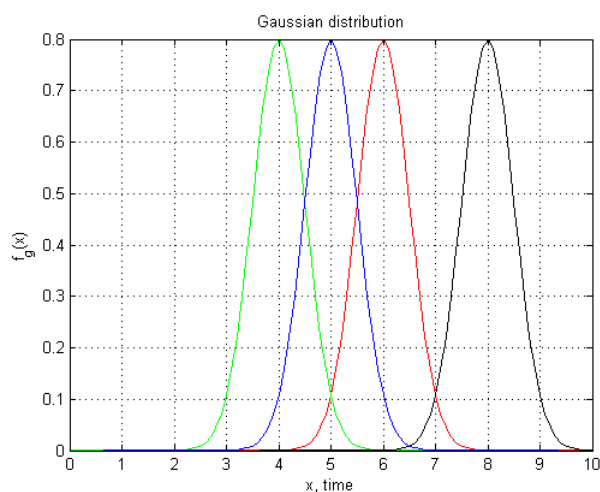


FIGURE 2.15: Four different Gaussian distributions used to represent MUs

These four different Gaussian distributions (MUs) are spatially distributed at different regions in the SR image. Figure 2.16 shows the chosen regions, where two of the motor units, 2.16(a) and 2.16(c), overlaps in space. All the MUs overlaps to some extent in time, so this example can be seen as an ultrasound SR sequence containing one contraction where four MUs are innervated.

Before taking the SVD of the SR sequence, the SR sequence has to be transformed into a zero mean 2D-matrix,  $X$  (Figure 2.11). In this test case, the dimensions of the SR data is  $150 \times 60 \times 101$ , which after conversion is a  $9000 \times 101$  data matrix ( $X$ ). Performing SVD on this  $X$ -matrix gives the two column-orthonormal matrices,  $U$  and  $V$ , and the diagonal matrix  $S$  that contains the singular values.

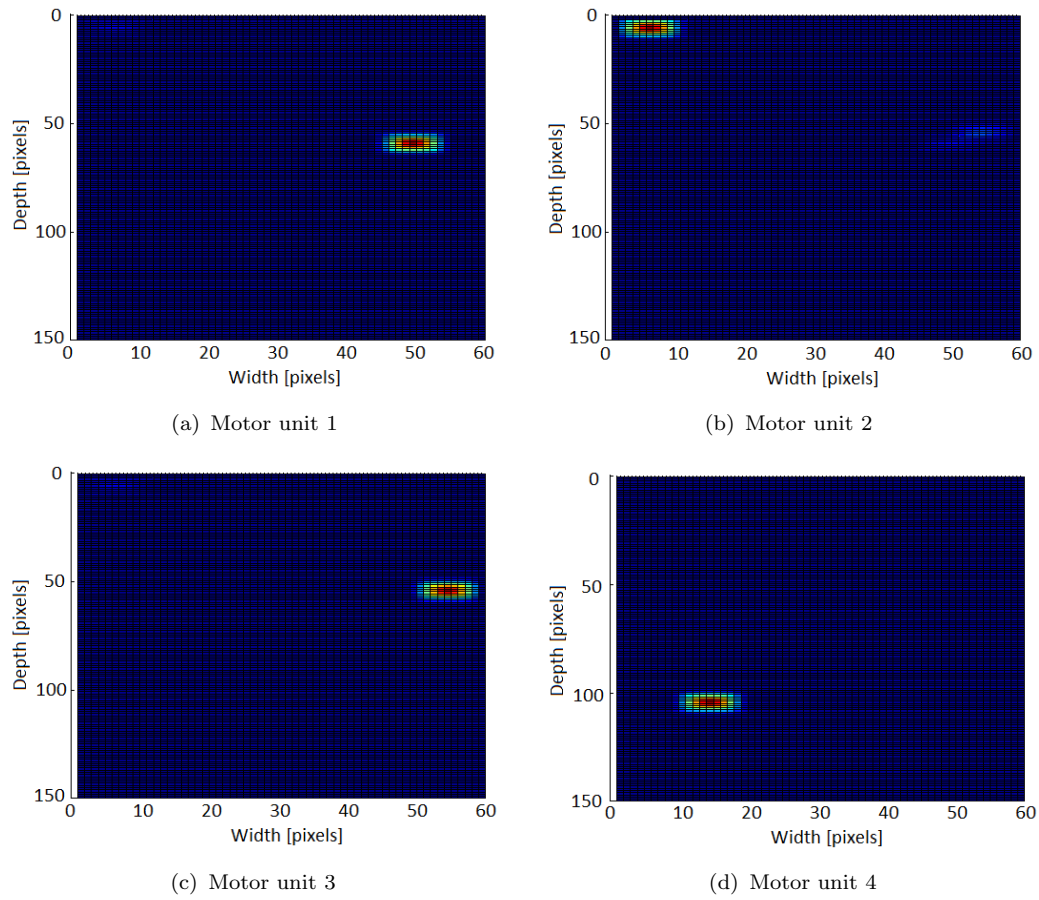


FIGURE 2.16: Images showing the location of the four motor units.

The column vectors in the  $U$  matrix are the PC directions of the data matrix  $X$ . The first column is the vector that coincides with the biggest singular value, the value that represents the biggest variance. The first column can therefore be seen as the image that differs most from the normal.

By computing the energy of this  $S$ -matrix, the energy function in Figure 2.17 is obtained. As seen, only four PCs are needed to represent the image sequence of 101 frames with 100% accuracy. With three PCs, it is possible to reconstruct the image sequence with a accuracy of 86.95%. In this example, only three PCs are used to be able to visually interpret this method.

By plotting the three leading column vectors of  $U$  against each other and the three leading column vectors of  $V$  against each other, the Figures 2.19 and 2.20 are obtained, respectively. Since the location and the activation time of the MUs

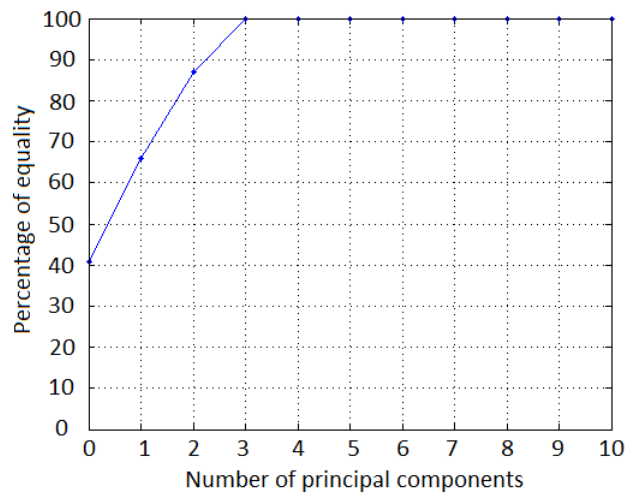


FIGURE 2.17: Energy function

are known, their assigned regions are plotted with different colors in these two images.

Each column in the  $U$  matrix represent an image, so each point in Figure 2.19 can therefore be seen as pixels. Since the data matrix  $X$  is zero-mean, most of the pixels will be situated in the origin, as seen on the projection of the pixels (black dots) in Figure 2.19 and Figure 2.20. The three leading PC directions are plotted against each other, so if there are pixel values different from zero in one of the PCs, these pixels will extend away from the origin. Figure 2.19 displays this effect, where all the regions containing contractions are extended from the origin. In the background, all the values from the PCs are plotted in blue, to show that the extracted regions will overlap the pixels that extends from the origin.

The four leading PCs are shown as SR images in Figure 2.18. It is seen that all MUs are captured by the three leading PCs and since "Motor unit 1" and "Motor unit 3" are present in both the first and third PC, they expand along both "Principal component 1" and "Principal component 3" in Figure 2.19. Some pixels are still blue in the region of the three first "Motor units", which is expected when looking at the fourth PC in Figure 2.18(d), where "Motor unit" 1, 2 and 3 are present. Four PCs are needed to represent the original data, but three PCs are still sufficient for showing this method.

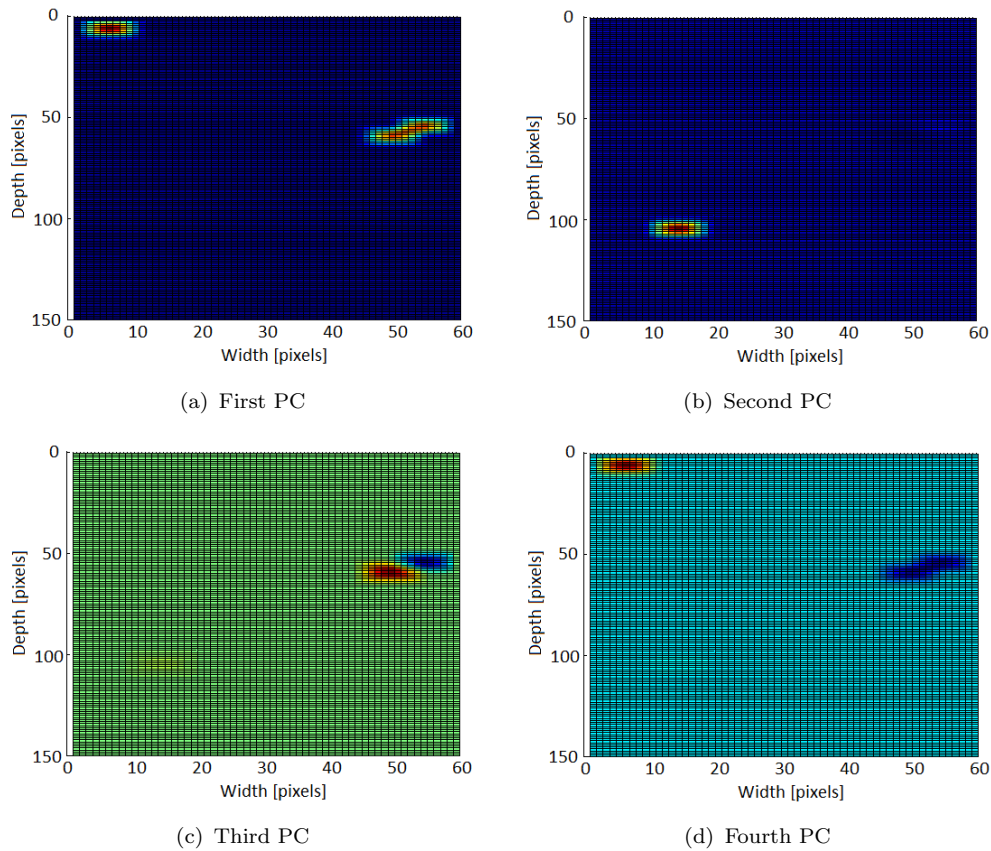


FIGURE 2.18: SR images of the four leading PCs

The plots in figure 2.19 and 2.20 can not be interpreted alone. Figure 2.20 shows "how much" activity there are at a given time (score per time). The numbers on the graph displays the time, while the extent from the origin shows the score. So if the graphs in Figure 2.19 and 2.20 does not expand in the same direction, it is an indication of no present MU activity. If the two figures are compared, it is seen that the coloured graphs extends in the same regions in both images and that the "Motor units" overlaps in time, which is expected, since the Gaussian distributions in Figure 2.15 overlaps.

If it is possible to classify the clusters (MUs) based on their extension from the origin and connected points (pixels) in 2.19 and 2.20, it may be used to locate individual MUs in a sequence of ultrasound SR images.

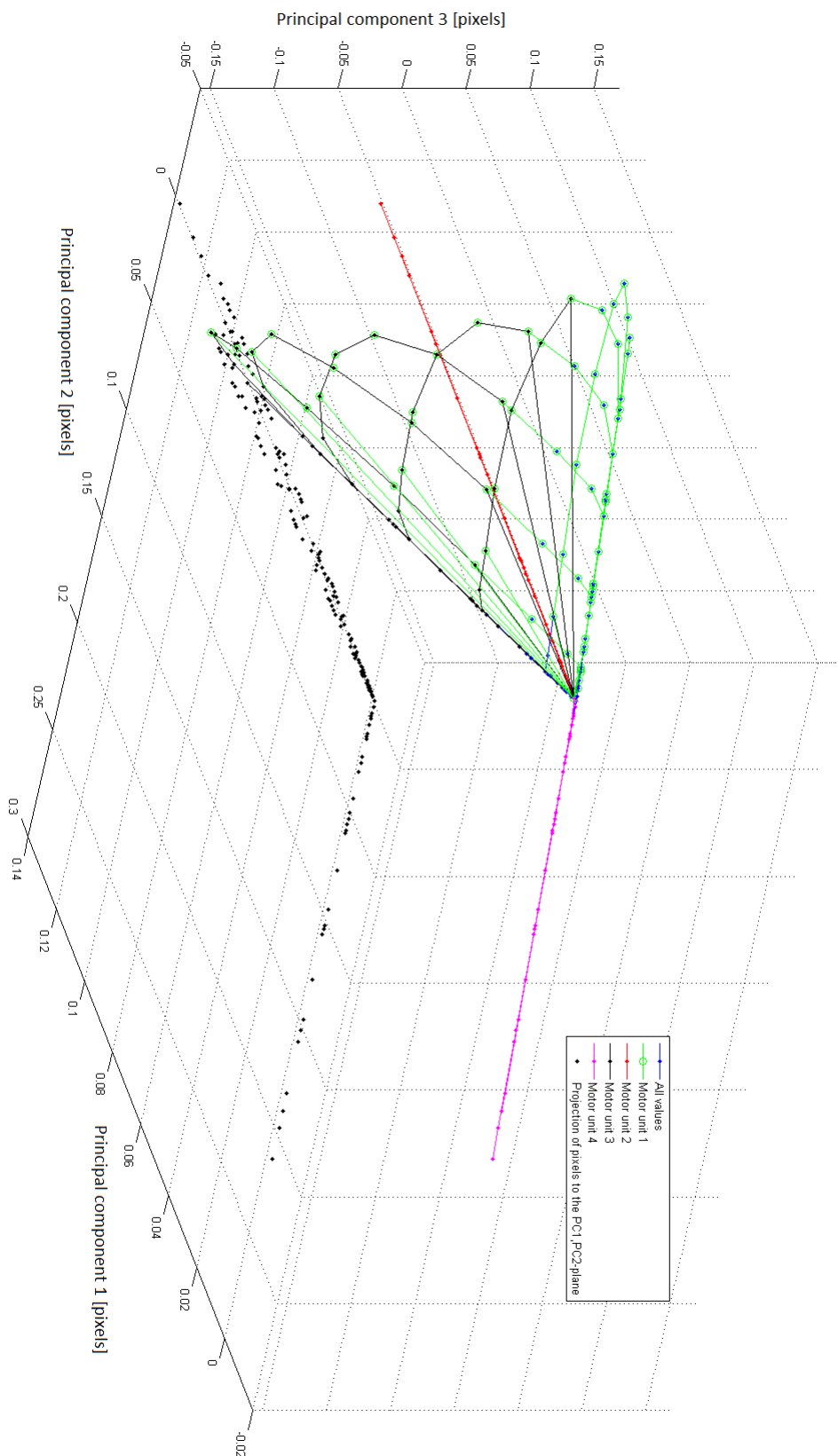


FIGURE 2.19: Plot of the three leading PC directions in  $U$  (pixels)



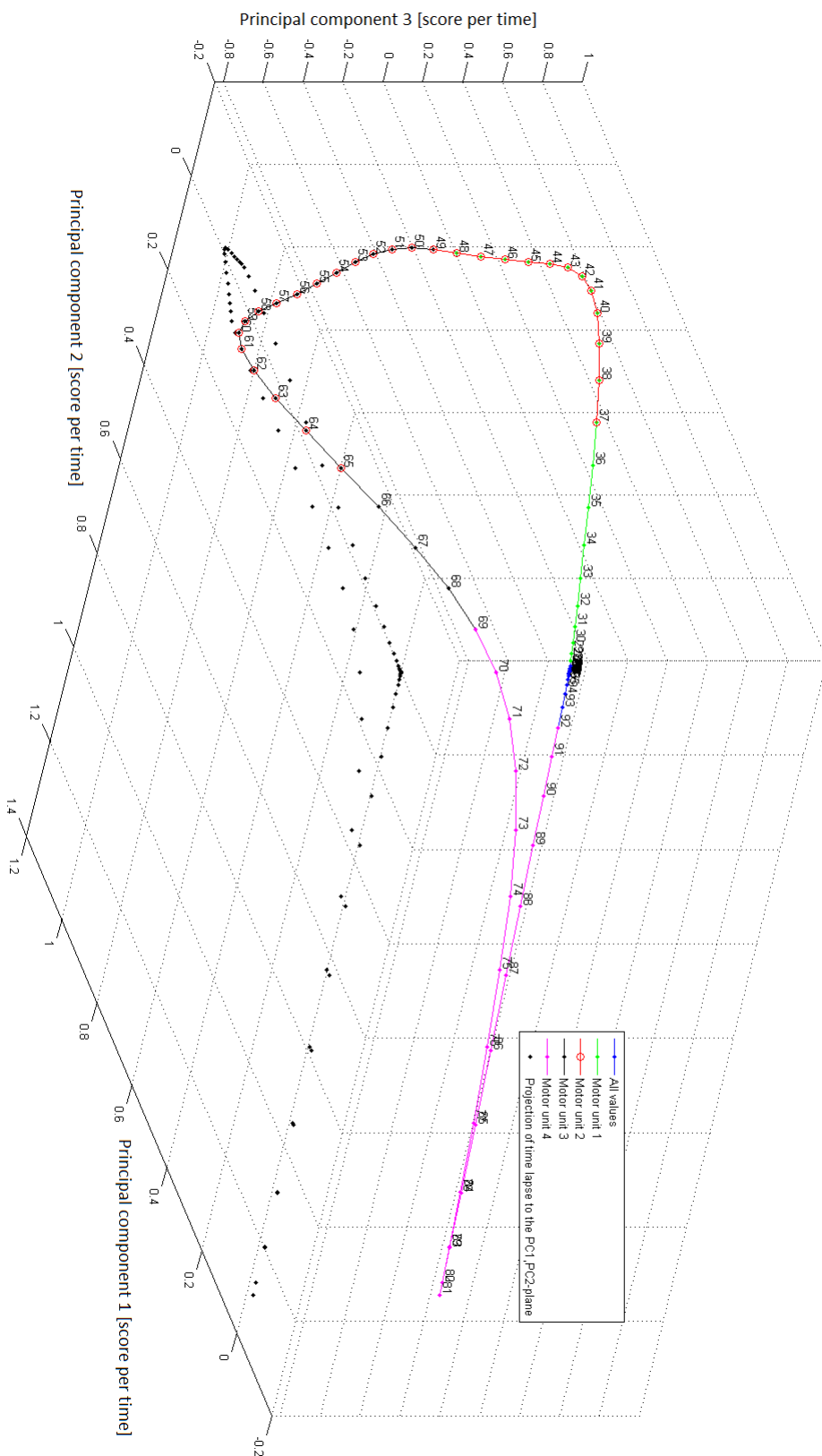


FIGURE 2.20: Plot of the three leading PCs of  $V$  (score per time)



# Chapter 3

## Methods and implementation

This chapter addresses the methods used in the implementation of the programs and contains information about used equipment and why this equipment is the optimal choice for measuring muscle activity using ultrasound.

### 3.1 Loading ultrasound raw-data in MATLAB

The program for loading ultrasound raw-data into MATLAB (mUDT) were received from St. Olavs Hospital. It is a protected time-limited MATLAB file which have to be renewed every six months. The program can be used to transform ultrasound B-mode, TVI and ECG data to be compatible for MATLAB analysis. The ultrasound data can be either IQ or RF data, depending on how the raw-data was stored on the ultrasound scanner. Most of the raw-data used in this project is from M. Heger (2013) [8], which was stored as RF-data. The MATLAB codes for this project therefore requires the use of RF-data.

The mUDT program takes raw-data as input and makes an mUDT class object that contains all information from the raw-data and is usable in MATLAB. Figure 3.1 shows a class digram for the program and what kind of outputs it is possible to extract from the object. As seen in Figure 3.1, four of the functions listed in

the mUDT class object are the same, but with different function calls, which leads to each of the four structs: Bmode, TVI\_auto\_corr, TVI and ECG.

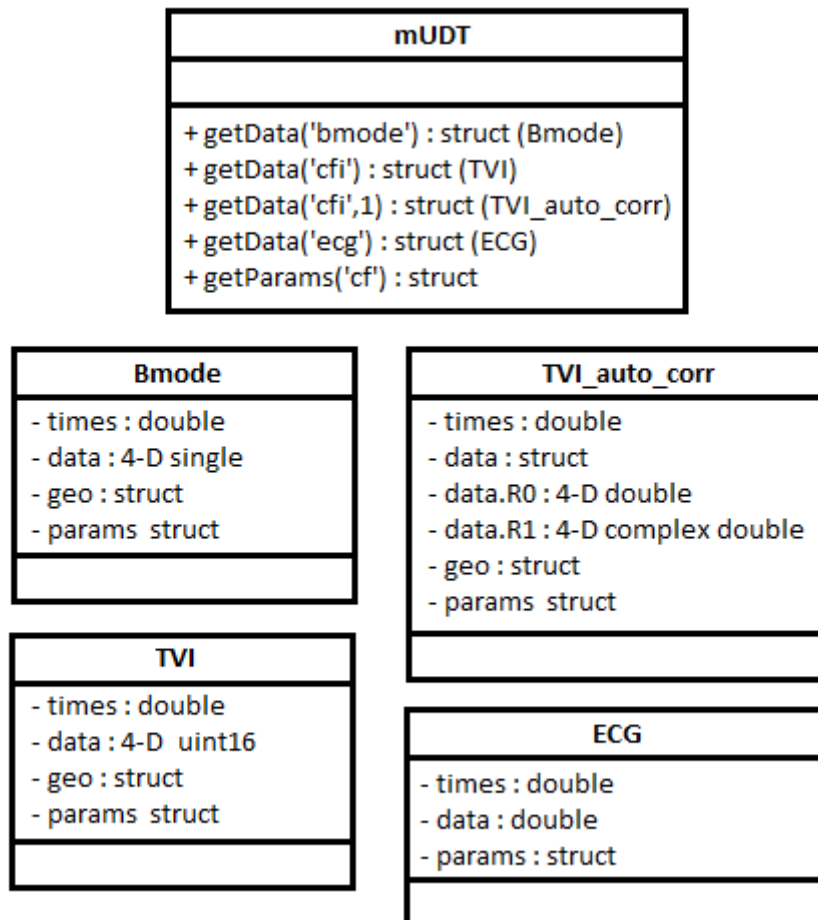


FIGURE 3.1: Class diagram for the mUDT program

When extracting TVI data, there are two different options that can be used, called TVI or TVI\_auto\_corr in the class diagram in figure 3.1. It can either be a displayable brightness image (TVI), or in the form of the autocorrelation estimates with no lag (R0) and lag 1 (R1) (TVI\_auto\_corr). The latter is what is used in this project to be able to calculate the velocity field and SR.

Extracting B-mode data is only useful for displaying a typical gray-scale image of the ultrasound image, but this data has an FR equal to the ultrasound scanner monitor which is only 60Hz and is therefore not usable for calculating SR.

## 3.2 Equipment and test setup

The equipment for the time delay experiment is in accordance with earlier experiments which consists of a GE Vingmed Vivid E9 ultrasound scanner with an ML6-15 linear probe. High resolution and high FR is crucial to locate small and fast changes in muscles. The scans was executed at depths between two and four *cm* and linear probes are preferable for superficial scanning, since it is possible to operate with high frequency to increase resolution and FR without much attenuation. To get as high FR as possible, the test-option "Msc TVI" (Muscular TVI) in "strain rate"-mode with a frequency of 15MHz was the chosen option.

Table 3.1 shows the chosen scanner, probe and scanner settings. The optimal PRF was not examined in the experiments from M. Heger (2013) [8], so the experiments in this study will use the same PRF, even though this PRF might not be optimal for the given task.

Scanner:	GE Vingmed Vivid E9
Probe:	ML6-15
Option:	Msc TVI
Mode:	Strain Rate mode
Frequency:	15MHz (maximum)
Strain length:	2mm
PRF:	750Hz
Depth:	2-4cm
Frame rate:	120-220 fps
EMG electrodes	ECG electrodes on VE9 scanner
Number of pulses:	3

TABLE 3.1: Test equipment

To localize and classify individual MUs, raw-data gathered from M. Heger [8] was used and the equipment listed in Table 3.1 were also used in [8]. To image muscle activity using ultrasound, the probe was placed in a fixed position over the anterior side of the upper arm, with ECG electrodes placed on each side of the probe for

detection of MUAPs. The probe were placed distal to the muscle belly, because the muscle belly contains most of the neuromuscular junctions. The experiment for measuring time delay between ECG electrodes and ultrasound response uses the same equipment, but different execution, described in the next chapter.

### 3.3 Time delay between ECG electrodes and ultrasound response

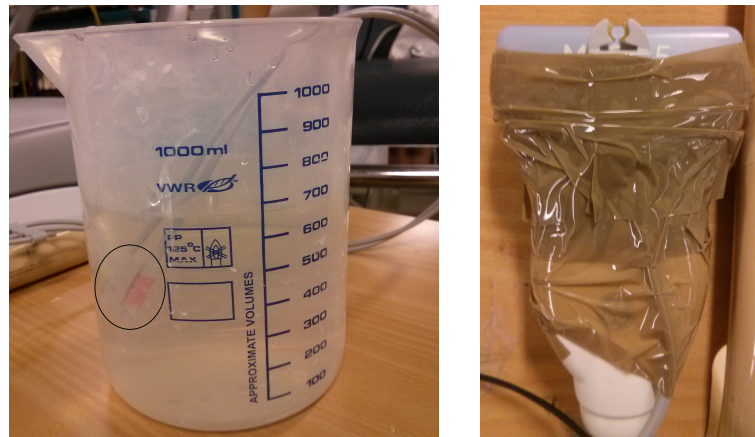
#### 3.3.1 Test setup and experiment execution

Earlier scans from M. Heger [8] were executed at different depths, hence different FRs. The time delay test is therefore also executed at five different depths and categorized in six groups of FR intervals. Because the sampling frequency for the ECG is higher than for the ultrasound scan, some small delay will almost always occur. The size of this time delay will depend on the ultrasound scans FR. A table containing expected delay due to difference in sample frequency can be seen in table 3.2.

Depth [cm]:	4	4	3.5	3	2.5	2
Frame rates:	126	194	200	207	213	221
Sampling intervals [ms]:	7.94	5.15	5	4.83	4.69	4.52
Expected time delays [ms]:	3.97	2.58	2.5	2.42	2.35	2.26

TABLE 3.2: Expected time delays

The experiment were executed by placing two of the ECG electrodes in a bucket of water and attach the last electrode to the probe by the use of tape, like the images in Figure 3.2. While recording, the probe was quickly submerged in water. This resulted in an ECG electrode and ultrasound response equal to the response in Figure 3.3 and 3.4, respectively. It is important that the tip of the electrode is aligned with the probe footprint to make it easier for the electrode and probe to react at the same time when submerging the probe in a directly vertical motion.



(a) Bucket containing water and ECG electrodes (marked with a circle)

(b) ECG electrode attached to ML6-15 probe

FIGURE 3.2: Test set-up for measuring time delay between ECG and ultrasound

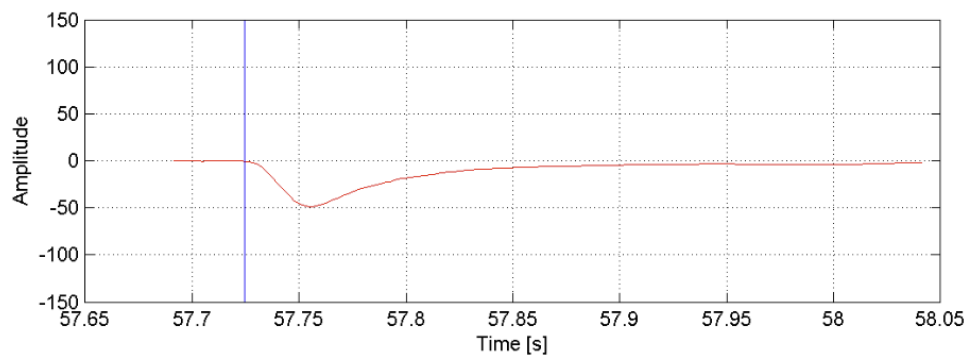


FIGURE 3.3: ECG response when submerging electrode in water, with a vertical blue line showing when the ECG electrode reacts to the water.

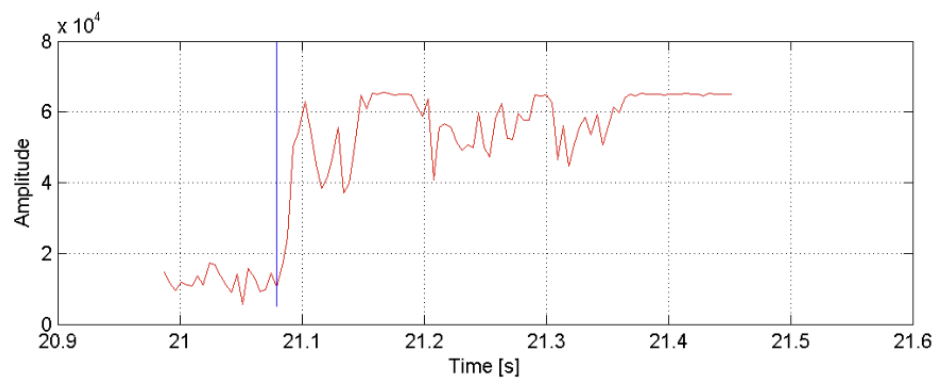


FIGURE 3.4: Ultrasound response when sinking probe in water, with a vertical blue line showing when the probe reacts to the water.

### 3.3.2 Problems

There are a couple of problems with this method. The ECG electrodes is made for measuring a continuous heartbeat and not completely suitable for this kind of testing. The electrodes are dependent of motion and goes to "sleep"-mode if some kind of motion is not present. After making the electrodes react, they must be at rest and the probe needs to be submerged quickly for the test not to fail. In addition to this problem, it is difficult to submerge the probe exactly vertical by human motion, which makes it difficult for the electrode and probe to hit the water simultaneously. Since the probe is quickly submerged, this should not influence the measurements to a large extent.

### 3.3.3 Program for calculating time delay

Figure 3.5 shows a flow chart for the program that calculates the time difference between ECG data and ultrasound image response. Under is a list explaining what happens in each block in the flow chart.

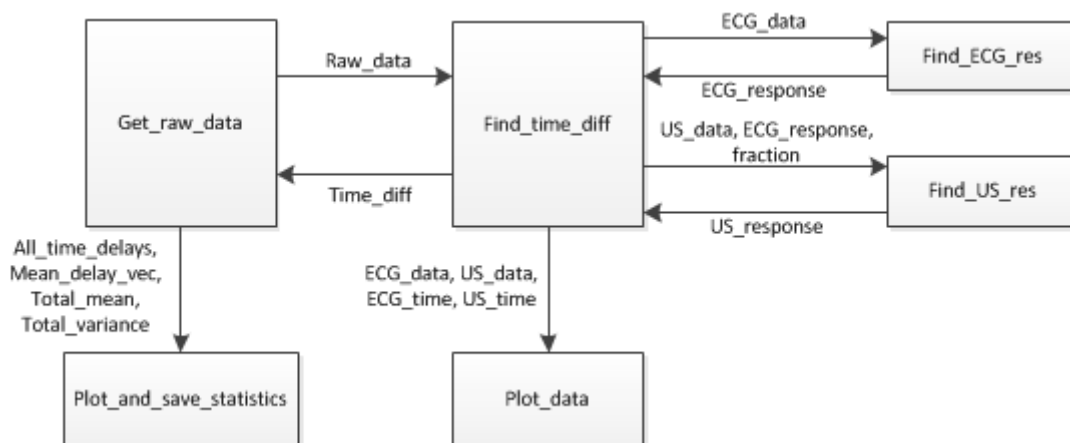


FIGURE 3.5: Flow chart for time delay calculation program

- `Get_raw_data`: This file starts the program by searching for and making an object of the raw-data by using the `mUDT` program got from St. Olavs Hospital. It iterates through all the folders in the directory containing the



raw data and runs the `find_time_diff` for each raw data it finds. After going through all the raw-data for each FR, all the time delays is recorded in a vector to find the mean value and variance. All the time delays independent of FR is recorded in a separate vector to find the total mean and variance, which can be used if the time delay is independent of FR.

- `Find_time_diff`: This function takes raw data as input and returns the time difference between ECG data and ultrasound image response.
- `Find_ECG_res`: Takes `ECG_data` as input and returns the sample number of the start of the ECG pulse. The start is found by taking the cross correlation between a known ECG response and the ECG sequence from the given raw-data. The peak index of the correlation sequence after halving gives us information about where the known ECG sequence overlaps the most with the new ECG sequence.
- `Find_US_res`: Returns the sample number of the start of the ultrasound response. Since the ECG electrode is located in the center of the probe, the ultrasound data is processed by picking out the eleven middle vertical lines and taking the mean value of all the data points in this limited rectangle. This is done for each frame, which gives a response equal to the sequence in figure 3.4. The `US_response` is found by searching for a slope that increases with at least 15000 in the next two steps. Because the response is so fast, it did not seem that filtration would be advantageous and slope search seemed to be sufficient for the task.
- `Plot_data`: This function plots the `ECG_data` and `US_data` with a vertical line marking the start of the responses, which is shown in Figure 3.3 and 3.4, respectively.
- `Plot_and_save_statistics`: This function gives three different plots for interpreting the statistical data of the time delay.

## 3.4 Program for motor unit localization, Localization\_auto

The program for MU localization uses multiple sub-programs and the layout for the main program is shown in Figure 3.6. As shown in Figure 3.6, it is the "Localization\_auto" program that is the start. This program finds raw-data automatically by searching through a given directory. Each of the sub-programs are run sequentially after the number in each box. Figure 3.7, 3.9 and 3.11 shows the layout for program 4, 5 and 6 in Figure 3.6, respectively. Each sub-section in this section gives a description for the functionality of each of these functions, while the MATLAB codes located on the DVD contains commenting describing both functionality and variables.

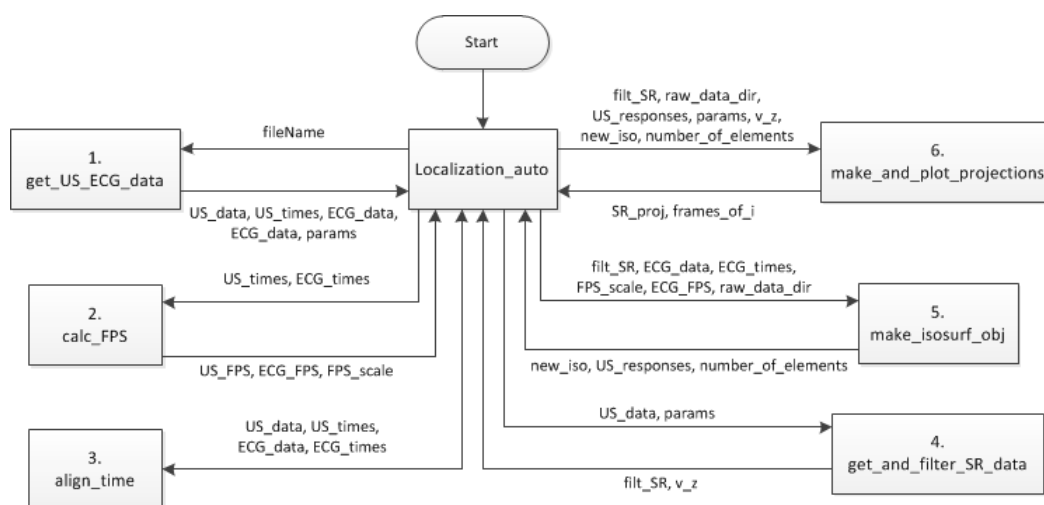


FIGURE 3.6: Localization\_auto program layout

### 3.4.1 Synchronization of ECG and ultrasound sequence, align\_US\_ECG

Recorded EMG and ultrasound data are almost never synchronized, which means that the start and end time for the EMG and ultrasound sequence are not the same. To solve this problem, a program was made to detect which data sequence

that starts and ends first and then remove the parts that are outside this time interval.

### 3.4.2 Get and filter strain rate data, `get_and_filter_SR_data`

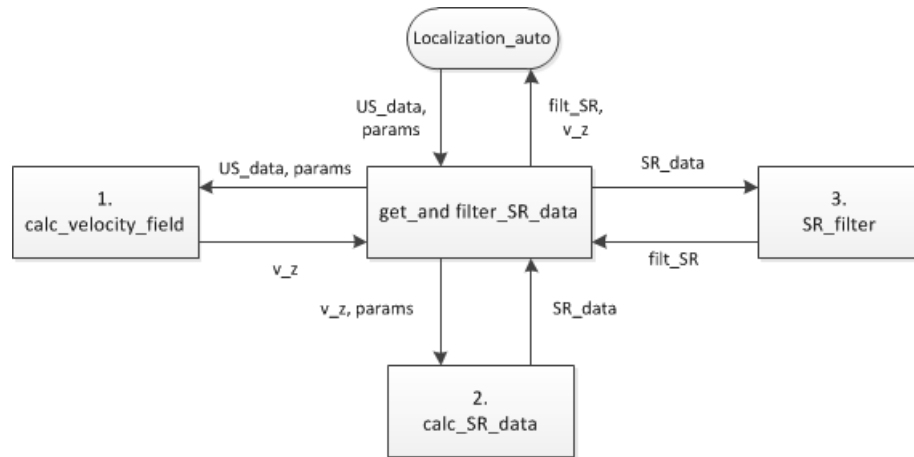


FIGURE 3.7: `get_and_filter_SR_data` program layout

### Velocities and strain rate in ultrasound image, `calc_velocity_field` and `calc_SR_data`

The velocity field of the ultrasound sequence was found by using formula 2.11. This formula uses the autocorrelation estimate with lag 1 (R1), which is automatically extracted from the `mUDT` class object. The frequency and PRF variables used to calculate the velocities in the program is extracted from the parameter list from the `getParams`-function from the `mUDT` object and is therefore the same as when the scans were executed.

Ultrasound SRI is based on the velocity gradient as explained in Chapter 2.3.5. To find the SR, the velocity difference between pixels has to be calculated. To reduce noise, the velocity difference is calculated between pixels with a distance equal to the strain length ( $\Delta x$ ) between each other. The program calculating the

SR sets the strain length to  $2mm$ , which means that the  $2mm$  closest pixels to the probe head gets excluded in the image. Some information gets lost, but since this is only  $2mm$  in the near field, it does not compromise the data to a great extent.

### Filters, SR\_filter

Due to a lot of noise in the SR images, so to get desired SR images, the SR images gets filtered with three different filters:

- Spatial filter: This filter is made as a weighted window filter. The weighting is based on the distance from the center pixel in the window, where the value is equal to  $\frac{1}{center+1}$ . The window size can be chosen, but since the SR images has better resolution in the axial direction, it is recommended to have a window that is higher than it is wider, like the one shown in Figure 3.8. A window that was nine pixels in height and seven in width was found to be preferable.

The drawback with this filter is that some information around the edges is lost. In example window in Figure 3.8, this will result in a loss of three pixels on the top and bottom part of each image, as well as two pixels left and right.

1/4	1/4	1/4	1/4	1/4					
1/3	1/3	1/3	1/3	1/3					
1/3	1/2	1/2	1/2	1/3					
1/3	1/2	1	1/2	1/3	→				
1/3	1/2	1/2	1/2	1/3					
1/3	1/3	1/3	1/3	1/3					
1/4	1/4	1/4	1/4	1/4					

FIGURE 3.8: Weighted spatial filter

- Temporal filter: The temporal filter is designed as a low pass butter-worth filter. The cut-off frequency were designed by averaging over a window containing a known contraction, finding the power spectral density (PSD) function and choosing a suitable cut-off frequency.
- Statistical filter: To remove unwanted small humps that are present throughout the SR images, the statistical filter removes values that are lower than the mean and standard deviation (STD) of the entire sequence.

### 3.4.3 Data representation and response to contraction, `make_isosurf_obj`

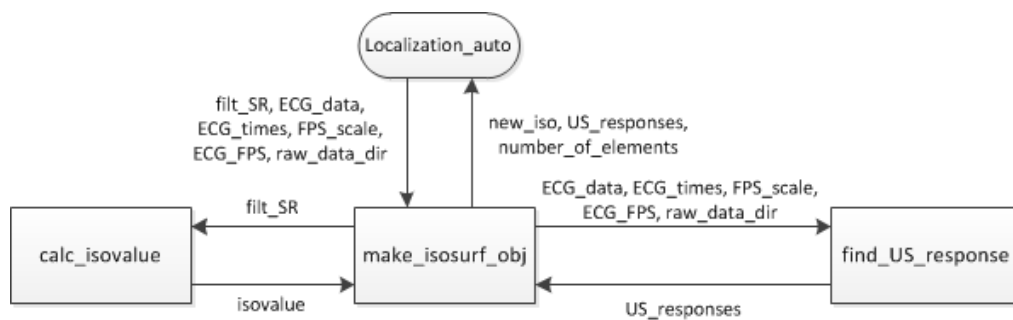


FIGURE 3.9: `make_isosurf_obj` program layout

To get a 3D-representation of the SR data, the "isosurface"-function in MATLAB was used. This function takes in the filtered SR data (`filt_SR`) and a parameter, `isoalue`, that in this case sets a threshold value for how great the SR has to be to be a part of the representation.

The "isosurface" object is a struct containing "vertices" and "faces". The "vertices" matrix are points in space, encapsulating contractions found by the "isosurface" function. This matrix is therefore used to locate contractions and mark it in the SR images. The "isosurface"-function contributes with both localization of muscle fiber activity and making a three dimensional plot of the "density" of the SR sequences.

### **Finding the isovalue, `calc_isovalue`**

The isovalue is found automatically by reshaping the SR data into a vector and finding the histogram for the data. After finding the histogram, the value that is most present in the sequence is found, and a percentage of  $3.67 * 10^{-4}\%$  of this value marks the wanted threshold for the isosurface function. This percentage was found by testing different isovalues based on the histogram of a known sequence of SR data. For each set of SR data, the closest value to the wanted threshold value is found, and the isovalue becomes the position (group) that contains this wanted threshold.

### **Detection of contraction using EMG data, `find_US_response`**

Detection of contractions from EMG data is done by the use of cross correlation. By loading a known EMG response of a contraction and cross correlate this response with the unknown EMG response, the output is a function with peaks that shows the time of arrival of a contraction. For a sequence containing one contraction, this peak is easily located by the maximum value in the output. For a sequence containing multiple contractions, the peaks are found by setting a threshold value that the peaks have to surpass to be counted as a contraction. In addition to this, the peak can not have neighbourhood peaks inside a region of 150 ms, which is the expected maximum time for a single muscle twitch. Figure 3.10 shows the result of this algorithm, where the known EMG sequence (pink) gets correlated with an unknown EMG sequence (red).

The blue vertical lines in the middle graph shows the chosen peak values from the cross correlation function. The second contraction marked by the cross correlation function shows the reason for checking the neighbourhood after peaks, since the first peak gets chosen even though it is lower than the next peak. The bottom graph showing the unknown EMG sequence indicates that this check is necessary, since the greater peak would result in a time later than the start time of the contraction.

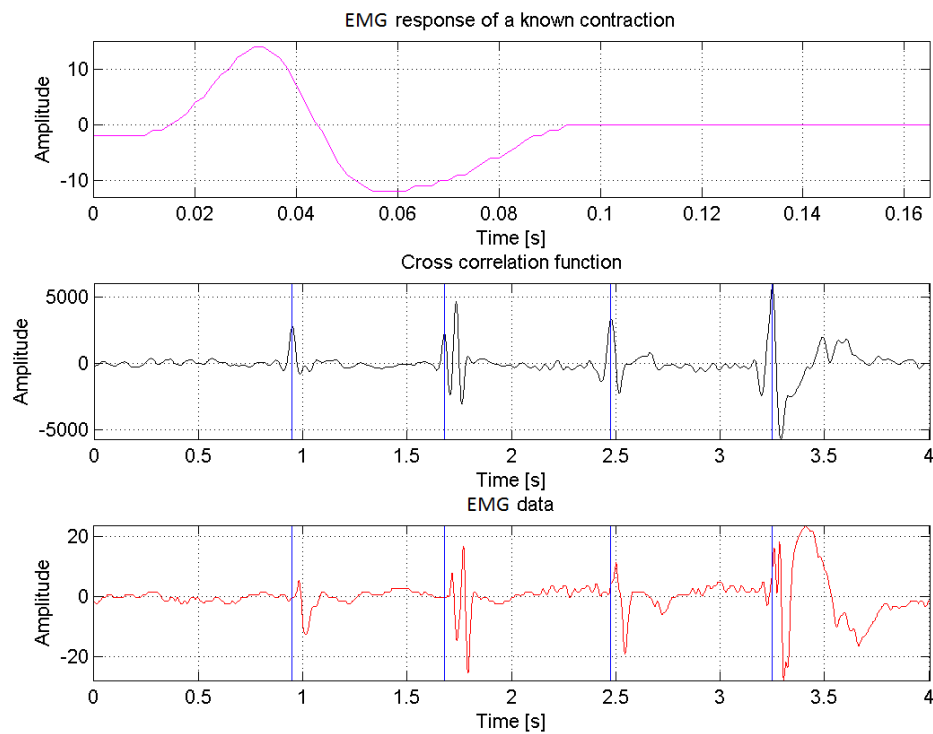


FIGURE 3.10: EMG data for locating start time of contractions

The returned vector from this function, "US\_responses", contains the frame numbers where contractions have been detected. This vector is used to exclude regions in the "isosurface"-object that is not a result from a known contraction seen in the EMG sequence. These regions is typically located near the start or end of the ultrasound sequence, where unwanted effects can occur due to movement of the arm when starting and stopping the recorded sequence.

### 3.4.4 Localization of regions of contraction, make\_and\_plot\_projections

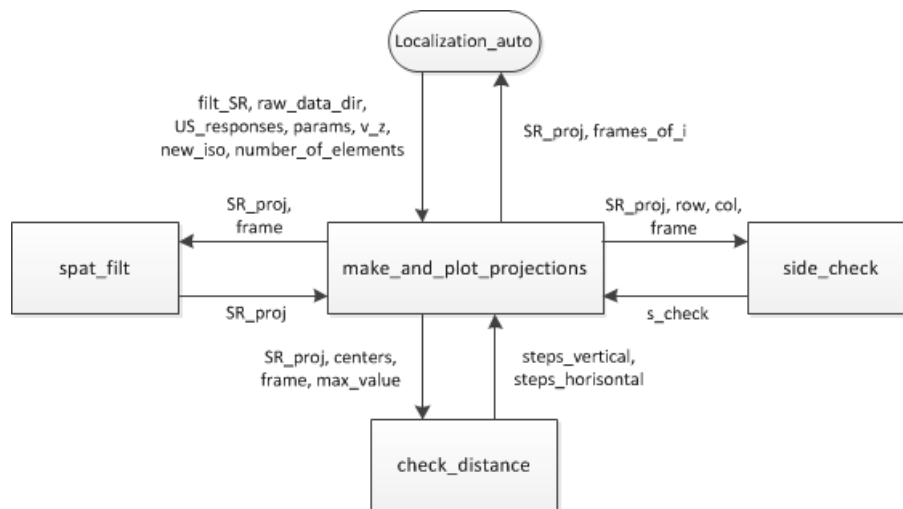


FIGURE 3.11: make\_and\_plot\_projections program layout

This program takes the output from `make_isosurf_obj` as input and use it to project the filtered SR data during a contraction to the depth-width-plane. All the frames belonging to a contraction gets integrated over before being projected, so if a sequence contains two contractions, two SR images are stored by this function.

#### Localization of muscle activity, check\_distance & side\_check

To locate regions of contraction, a search for all SR values at least 50 % of the maximum SR value in the image is done. The `side_check` function checks surrounding pixels to check if the found value is the maximum value in its neighbourhood. If the value is the largest in its neighbourhood, this value is stored. The area around these peak values are checked in the `find_distance` function to find the dissemination of the muscle activity. Images containing SR data with circles around the located regions of contractions are then stored.



## 3.5 Data reduction as a method for localization, feature\_extraction

### 3.5.1 Data reduction method

Based on the functionality of the different data reduction methods and classification methods proposed in Chapter 2.5 and 2.6, PCA in the form of SVD for feature extraction was the preferred option for a data reduction based MU localization algorithm. In addition to being able to localize MU activity, it is easy to use and one of the simplest methods presented in the theory chapter. The leading PCs of a zero mean filtered ultrasound SR sequence contains information of the position as well as the duration of the MU activity, as shown in the example in Chapter 2.6.

### 3.5.2 Program for feature extraction using SVD, feature\_extraction

A communication diagram for the feature extraction using SVD method is shown in Figure 3.12. The program is launched by running the feature\_extraction function and the function calls has to be done in the order of the numbers in the communication diagram.

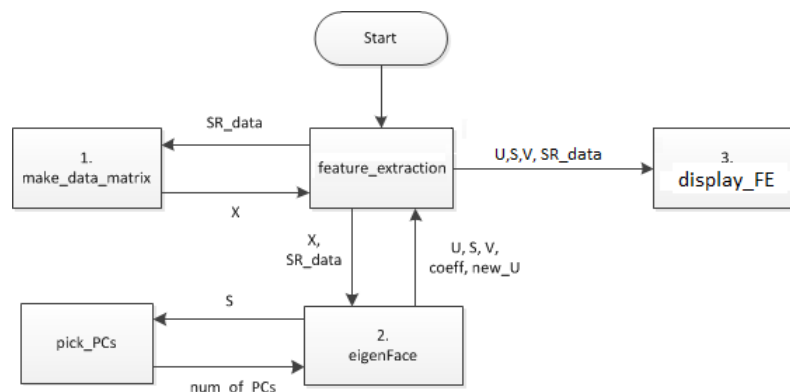


FIGURE 3.12: Communication diagram for the classification program

**feature\_extraction** sets the directory containing stored data from the localization algorithm and loads SR data.

**make\_data\_matrix** subtracts the mean from each frame in the SR sequence to make it zero mean and transforms it to a two dimensional data matrix  $X$ , according to Figure 2.11.

**eigenFace** takes the SVD of the data matrix  $X$  and calls upon the "pick\_PCs"-function which chooses a number of principal components ( $k$ ) based on the energy of the S matrix. The number of PCs should at least add up to 90% of the total energy of the S matrix, as stated in Chapter 2.5.3.

**display\_FE** plots the three leading PC directions against each other. The information about the centers and radii found by the Localization\_auto algorithm is used to display individual MUs in different colours to show how the "feature extraction using SVD" method works.

This program is not automatized, so the SR data that is going to be analysed by the feature extraction function has to be chosen manually. The centers and radii found by the "localization\_auto"-function gets saved and can be loaded into this program, but since this program is made to explain how this method works, manually selecting the regions based on the SR data that is analysed is sufficient.

It is also possible to set a window encapsulating the detected contractions, which is used to decrease the number of PCs needed to represent at least 90% of the dataset.

# Chapter 4

## Results and analysis

### 4.1 Time delay between EMG and ultrasound response

Table 4.1 shows the measured mean delay (MMD) and STD for each group of frame rates, where the "MMD - ETD"-field is "measured mean delay" minus the "expected time delay" due to the difference in sample frequency between ECG electrodes and ultrasound, shown in Table 3.2.

Frame rates:	126±1	194±1	200±1	207±1	213±1	221±1
Number of samples:	6	5	9	11	9	10
MMD [ms]:	4.63	4.02	5.84	5.24	4.52	5.27
MMD - ETD [ms]:	0.66	1.44	3.34	2.82	2.17	3.01
STD [ms]:	2.64	2.95	1.94	3.89	2.34	4.27

TABLE 4.1: Mean delays and standard deviation

The reason why there are different number of samples for each FR group is that a lot of data were not usable, because of bad response in either EMG or ultrasound sequences which were not noticed before loading the data in MATLAB. The reason for the  $\pm 1$  in each FR group is that a small increase in sample width will decrease

the FR and vice versa, so some variance in FR for each sample is present in the data set.

Table 4.1 indicates that the MMD is independent of FR, since the MMD does not consequently increase or decrease with respect to FR, even though the ETD is higher for lower FRs. Since Table 4.1 shows that the MMD is independent of FR, the total MMD and STD for all the 50 samples were calculated. The total mean delay was measured to be 5.06 ms and after subtracting the mean ETD, which is 2.68 ms, the time delay is estimated to be 2.38 ms. The STD of the complete data set was measured to be 3.11 ms.

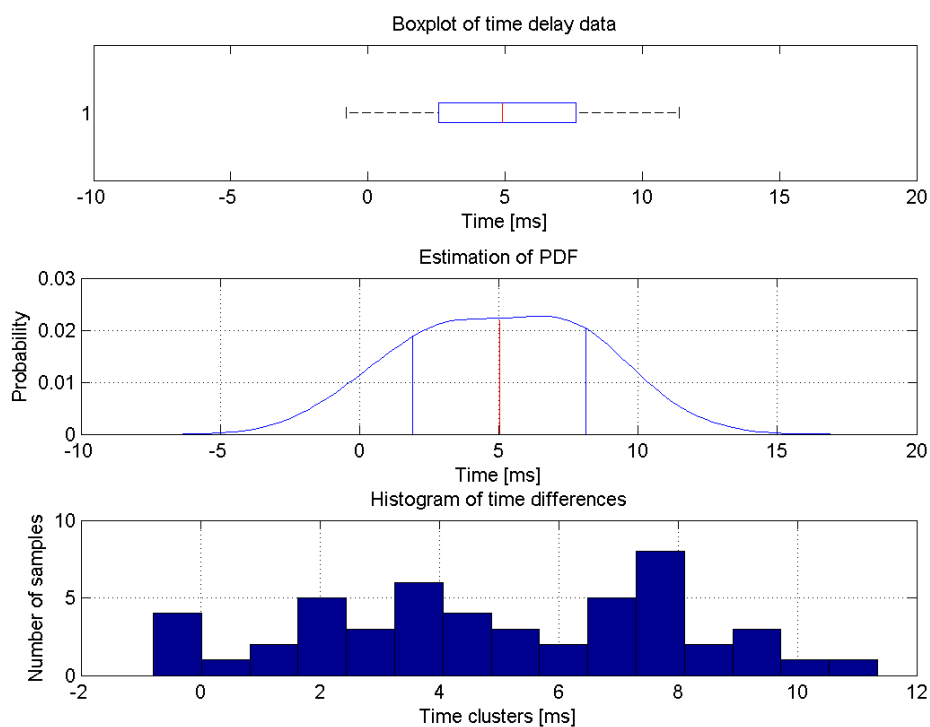


FIGURE 4.1: Statistical data for time delay between ECG and ultrasound response

Figure 4.1 shows three different ways of showing statistical data for the time delay independent of FRs. The red line in the two first plots shows the mean value of the data set, while the blue area in the box-plot is the area where 50% of the data

lies. The second sub-plot is an estimation of the PDF, made by the "ksdensity"-function in Matlab and seems to be a reasonable PDF with respect to the data, except that the tails seems a bit wide. The blue lines in the PDF indicates the area between -1 STD and +1 STD (1.98 and 8.13 ms), where 68% of the data lies.

The histogram shows that the intervals at -1 STD and +1 STD contains the most samples, which explains why the PDF estimation has two local tops. Four samples indicates that the ultrasound response is faster than the ECG response which should not be the case. The reason for this is most probably that the ECG electrodes is dependent on a continuous wave, explained in Chapter 3.2.2. This makes the ECG electrode react when it already is submerged in the water, which makes the probe react to the water before the ECG electrode.

A time delay of 2.38ms and STD of 3.11ms indicates that the time difference between ECG electrodes and ultrasound response is almost negligible. If a contraction is detected in an EMG sequence when scanning for muscle activity, the ultrasound response is expected to be seen after a certain time, equal to the delay caused by propagation velocity of the MUAP ( $EUD = 4.3 - 13ms$ ), in addition to the time delay between ECG electrode and ultrasound response. So the ultrasound response is expected to be seen between 6.68ms and 15.38ms after the EMG response.

## 4.2 Strain rate

To know that the SR measurements gives correct response, the SR data produced by the "calc\_SR\_data"-function after filtration is compared to the result from the Q-analysis tool on the ultrasound scanner. Figure 4.2 shows an example of the SR data calculated in MATLAB versus what is seen in the Q-analysis window on the ultrasound scanner. These two images are taken from the same ultrasound sequence which contains one contraction.

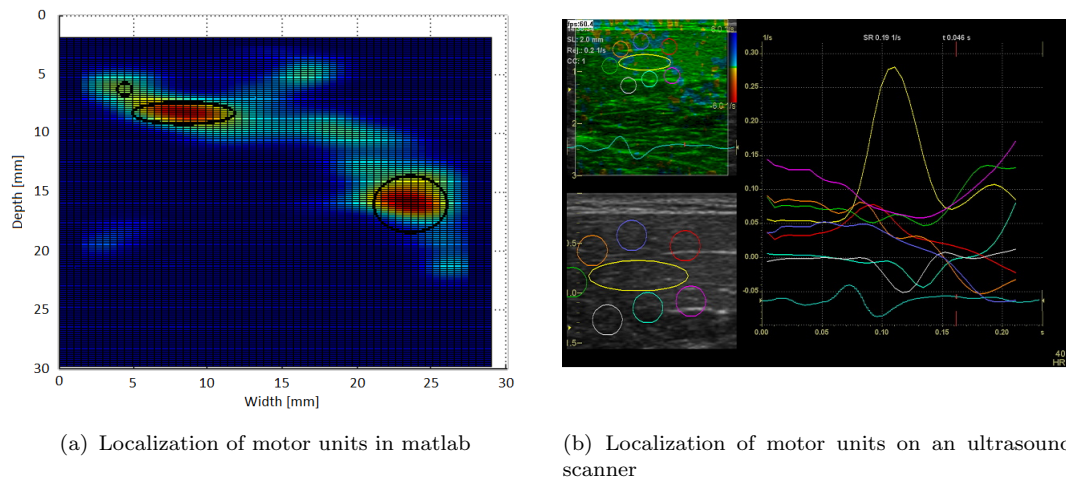


FIGURE 4.2: Localization of motor units

The SR image in 4.2(a) is the result from the "make\_and\_plot\_projection"-function, where all the frames during the contraction are integrated over and seen from the width-depth-plane (cross-section of the upper arm). These types of pictures will be referred to as projections of integrated SR images. As seen in Figure 4.2(b), the yellow region corresponds to the region between 7.5mm and 10mm in depth and between 5mm and 12.5mm in width in Figure 4.2(a).

The size of the detected regions of contractions is smaller than the maximum MUT, found to be 1cm by P. E. Barkhaus et al. (2013) [19], which may indicate that the detected regions are single MUs. Figure 4.3 shows two images from the same sequence as in Figure 4.2(a), where the upper image marks the time of the strain rate image at the bottom. If the SR image in figure 4.2(a) and 4.3 are compared, it is seen that the projection of the integrated SR images are not able to locate individual MUs. The MU located to the right in 4.2(a) is actually two different MU, which are visible in the surface plot in Figure 4.3.

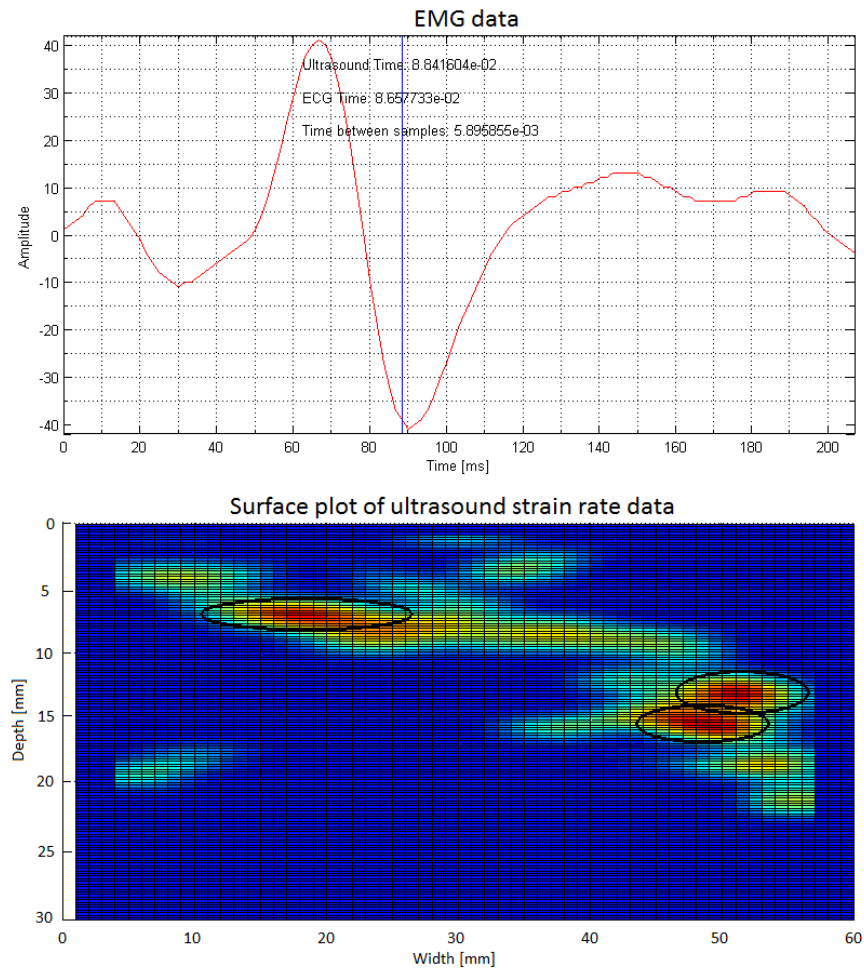


FIGURE 4.3: Strain rate image with ECG to shown time frame

## 4.3 Localization based on motor unit behaviour

### 4.3.1 Motor unit behaviour

To show how an MU behaves, a sequence of six image frames at six different times during a contraction is presented in Figure 4.4. The time for each of the six different frames are marked in Figure 4.5 with different coloured vertical lines.

As seen in Figure 4.4, the present MUs behaves as expected. After the contraction starts, the SR increases in the region of the motor unit before decreasing. The same conclusion can be drawn from the "isosurface"-objects shown in Figure 4.6, which shows a 3D representation of the SR sequence in Figure 4.4.

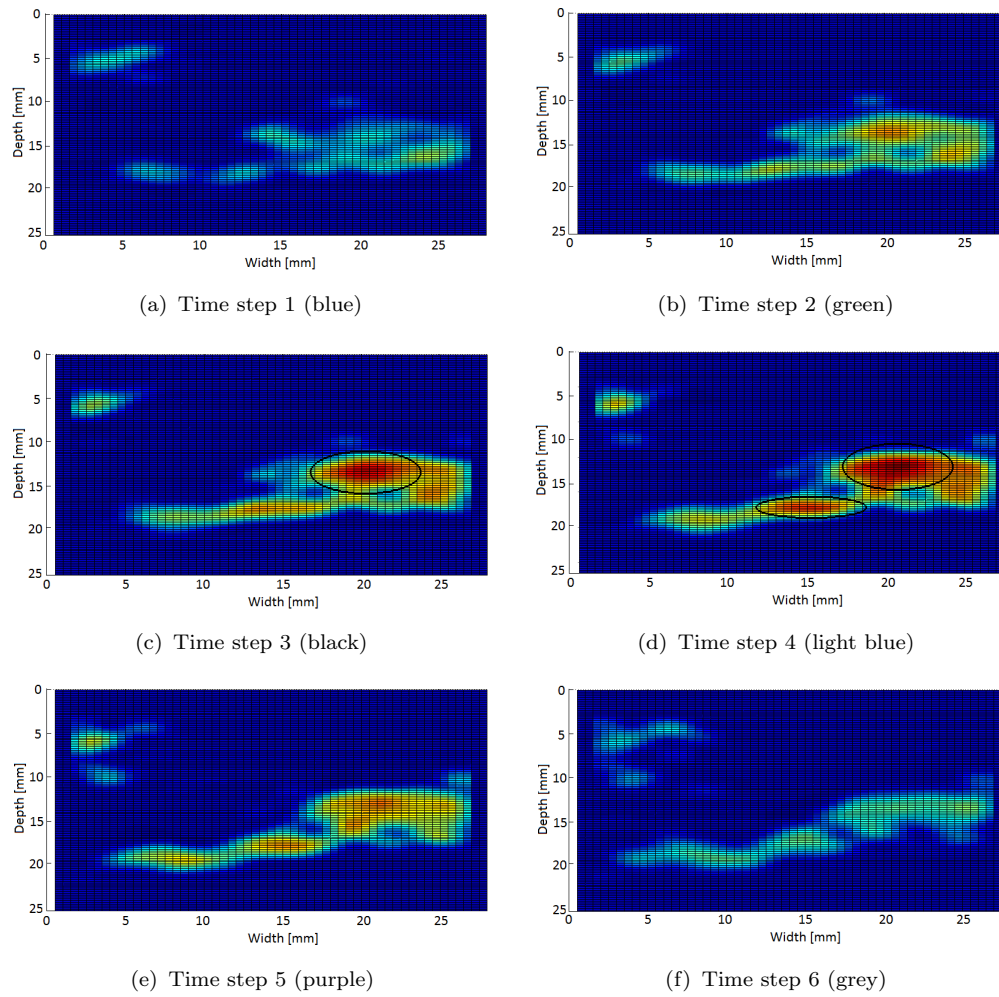


FIGURE 4.4: Six strain rate images showing different frames during a contraction

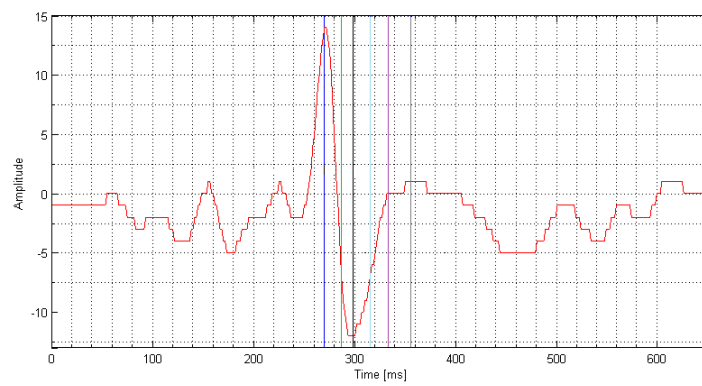


FIGURE 4.5: EMG response with marked time steps



In Figure 4.6(a), all the areas containing contractions happens a couple of frames after the detected contraction in the EMG sequence, which is at time "frames = 45". The yellow clusters in Figure 4.6(b) are located in the same regions showing contractions in the image sequence in Figure 4.4.

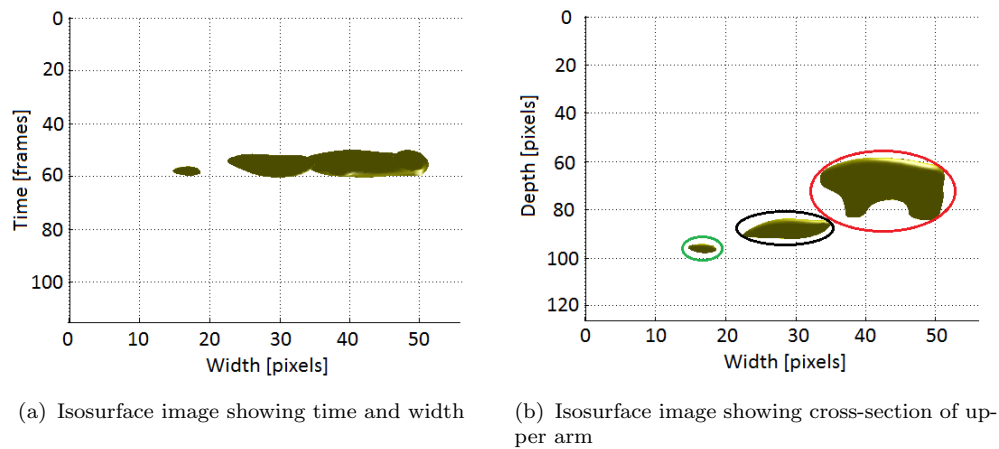


FIGURE 4.6: Isosurface images

### 4.3.2 Localization

To automatically detect regions of contraction based on MU behaviour, the "Localization\_auto"-function was used and an example of the result of this algorithm is shown in Figure 4.7, which is a projection of integrated SR images in the sequence shown in Figure 4.4.

Three MUs are detected in Figure 4.7. The same regions are encircled in the isosurface image in Figure 4.6(b) by using different colors, corresponding to the "Motor units" coloured in the next section (Figure 4.10(b)).

By looking at Figure 4.7, it seems that the region of contraction to the right is big, but inside the boundaries of an MU (1cm). It is also seen that this region is not circular, but it can still be a singular MU, since the MUT is not necessary a circle.

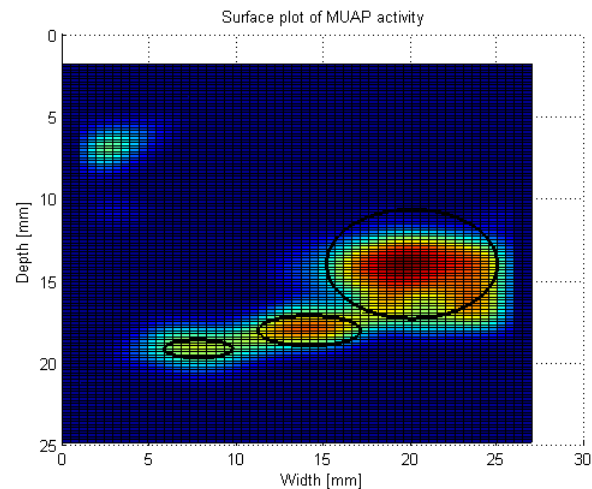


FIGURE 4.7: All strain rate images during a contraction added together

## 4.4 Feature extraction using SVD for localization of motor units

### 4.4.1 Ultrasound sequence containing one contraction

To show the result from the "feature extracting using SVD"-method, the same data set as in Figure 4.4 is used. Figure 4.8 shows the energy function for this dataset, which shows that six PCs are needed to represent over 90% of the data, but the three leading PCs adds up to 81.37% of the total energy, which is enough to make a good 3D-representation of the result.

The three leading column vectors (PCs) of the  $U$  and  $SV$  matrices are plotted against each other in Figure 4.10 and 4.9, respectively. Since the regions of contraction in the dataset is known, these three regions are picked out and displayed in three different colors in figure 4.10(b), corresponding to the coloured circles in Figure 4.6(b). As explained in chapter 2.7, most of the points are situated around the origin, which is seen on the projection of the graph (black dots) in Figure 4.10(a). The "motor units" in Figure 4.10 may not be individual MUs, but regions of contractions. They will still be referred to as MUs to ease the interpretation and analysis of the figures.

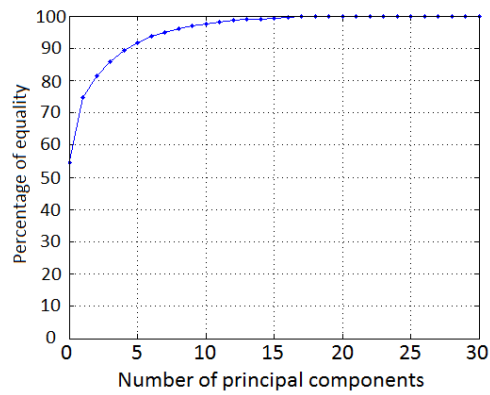


FIGURE 4.8: Energy function

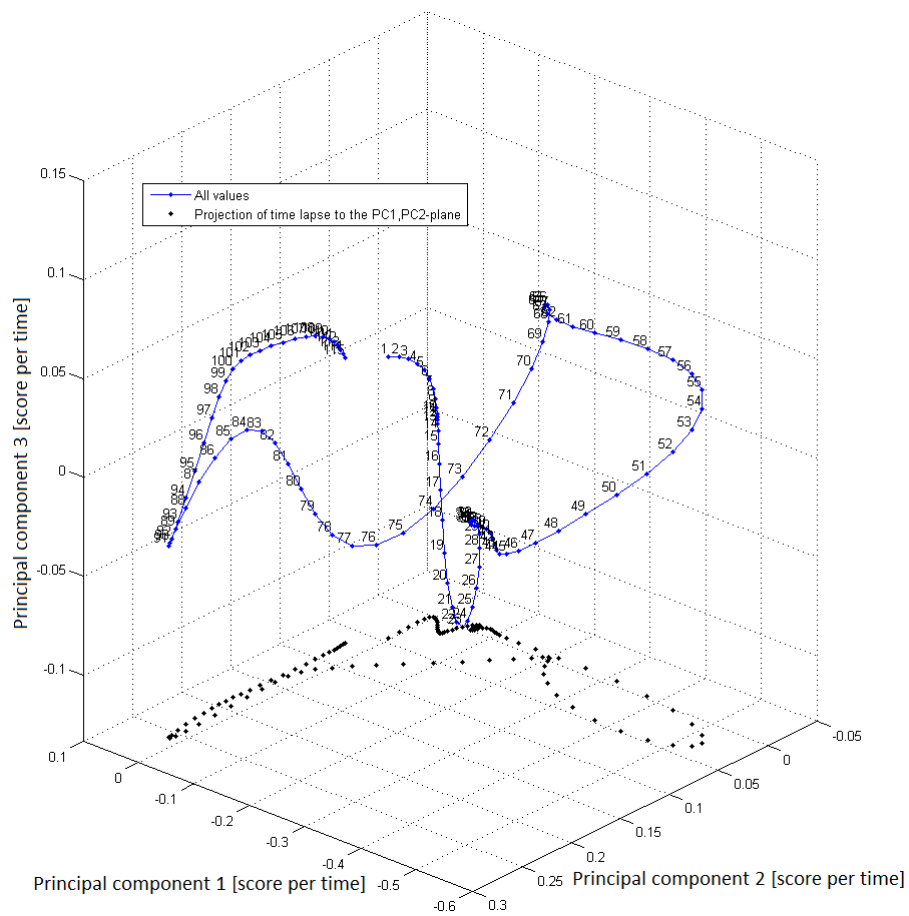


FIGURE 4.9: Feature extracting using SVD, activity at time steps

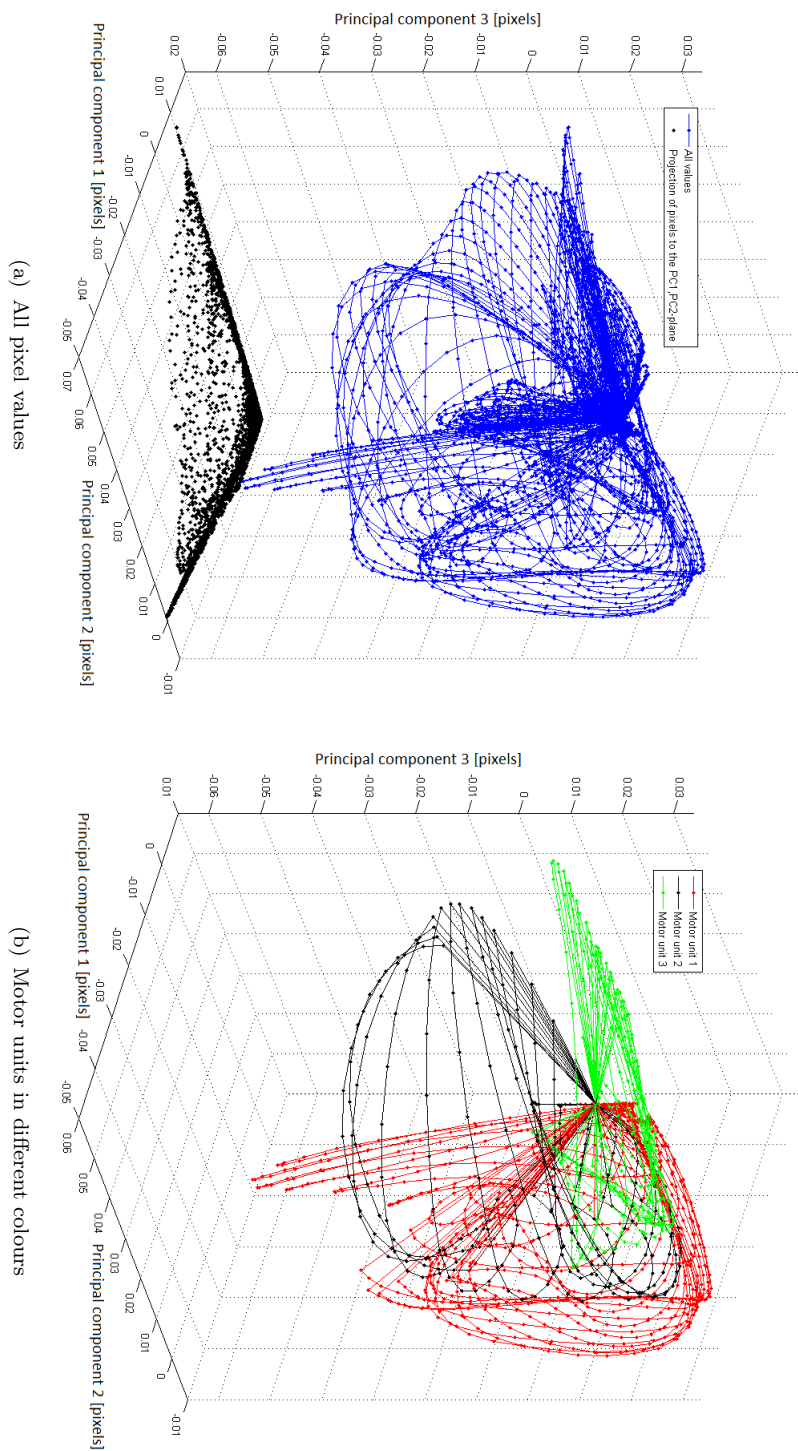


FIGURE 4.10: Feature extracting using SVD, pixels

The three "Motor units" (green, red and black) are clearly distinguishable when looking at Figure 4.10(b), but picking them out from Figure 4.10(a) is not straight forward. The red and green graphs are distinguishable, but it seems that there are another MU overlapping with the black region, in addition to a region that lies along the second PC.

The projection of the graph displaying the amount of activity for a given time (Figure 4.9) shows that there are much activity along the first and second PC, which corresponds to the red and green regions respectively. There are signs of activity in the black region as well, but less than for the green and red, which is expected based on the image sequence in Figure 4.4 which shows less activity in the black region.

Figure 4.11 shows the three leading PCs formed back into SR images. The second PC shows a region with a contraction in the upper right quadrant, which is not present in any of the images in Figure 4.4. There are signs of activity near the end of the SR sequence in this region, but this is because of probe lift when stopping the ultrasound recording. Based on the images in Figure 4.11, this "contraction" is the region that lies along the second PC axis in Figure 4.10(a), since this region is located in the upper right corner in image 4.11(b).

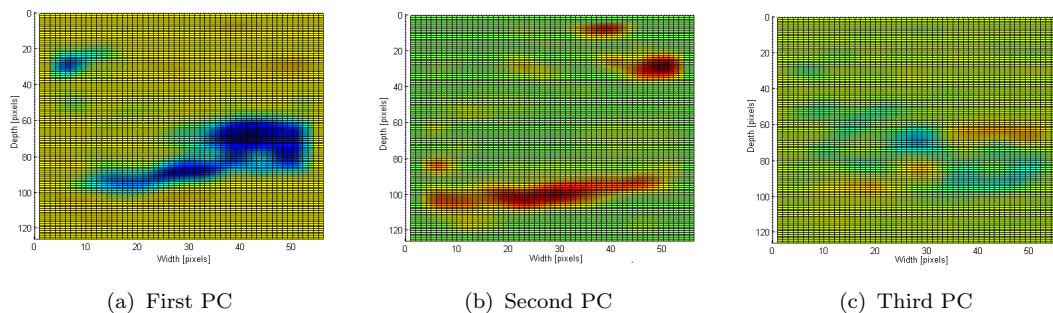


FIGURE 4.11: Strain rate images of the three leading principal components

It looks like it will be possible to localize individual motor units with the "feature extraction with SVD"-method, but because the sequence contains time steps before and after the contraction, there are some unwanted regions containing "contractions" that is a result from unwanted motion when starting and stopping the

ultrasound recording. In addition, four PCs are needed to represent at least 90% of the data, so it is difficult to visually illustrate this method. To illustrate this, a time window encapsulating the contraction has been picked out before taking the SVD of the sequence. The first PC in this case covered 91% of the total energy.

The 3D-representation of this is shown in Figure 4.13. The coloured regions (MUs) in Figure 4.13(b) now overlaps with almost all the pixels in Figure 4.13(a). This indicates that it may be easier to show to what extent the "feature extraction using SVD"-method works if the frames encapsulating the contraction captured in the EMG sequence is picked out before taking the SVD of the data.

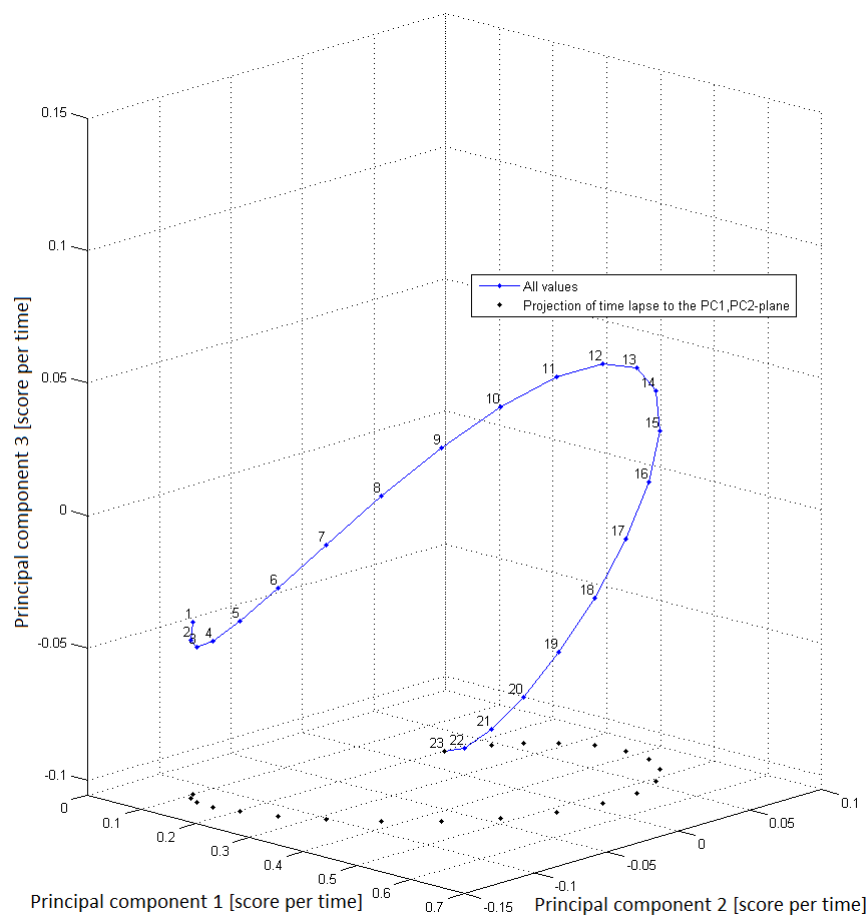


FIGURE 4.12: Feature extracting using SVD, activity at time steps

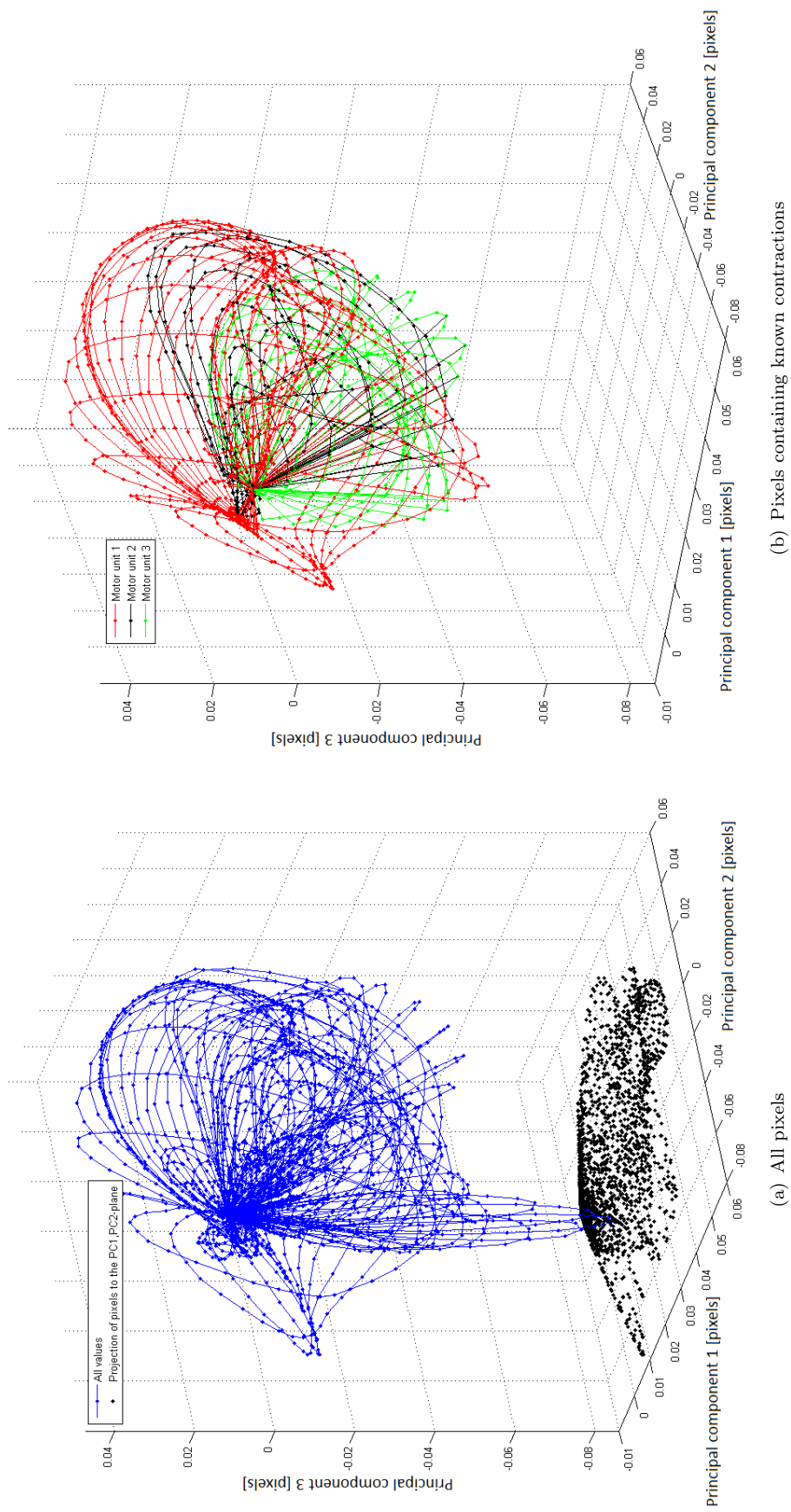


FIGURE 4.13: Feature extraction using SVD, pixels

Since this sequence only contains the encapsulated contraction, the graph showing score per time in Figure 4.12 is a simple arc, which spreads out in the same direction as the graphs in Figure 4.13. It is difficult to pick out the clusters in 4.13, but it is seen that all the "Motor units" are expanding from the origin, and by looking at connected dots (pixels), it should be possible to separate the three "Motor units".

#### 4.4.2 Ultrasound sequence containing multiple contractions

In this subsection, feature extraction is used on a data set containing four contractions. The EMG sequence for this dataset is shown in Figure 4.14, where the start of each contraction is marked with a vertical blue line. The four SR images in Figure 4.15 are surface plots showing the cross section of the upper arm, projections of integrated SR images.

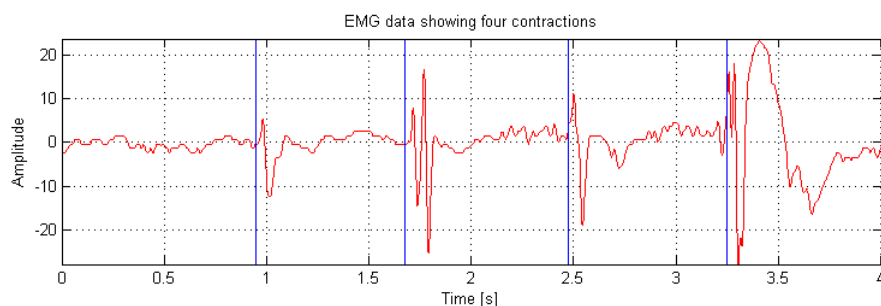


FIGURE 4.14: ECG sequence containing four contractions

From these SR images, it is possible to see where the individual MUs are located. As in the previous example, some regions that contains known contractions have been picked out. These regions are marked with coloured circles in 4.16 and the colour of the circle corresponds to the colours on the graph in Figure 4.18(b). This is a sequence containing multiple contractions and 818 frames and 24 PCs are needed to represent at least 90% of the energy. Because of this and the result found from encapsulating the contraction in the example in Chapter 4.4.1, the frames between contractions are removed, which resulted in a need for five PCs instead of 24 to represent at least 90% of the data.



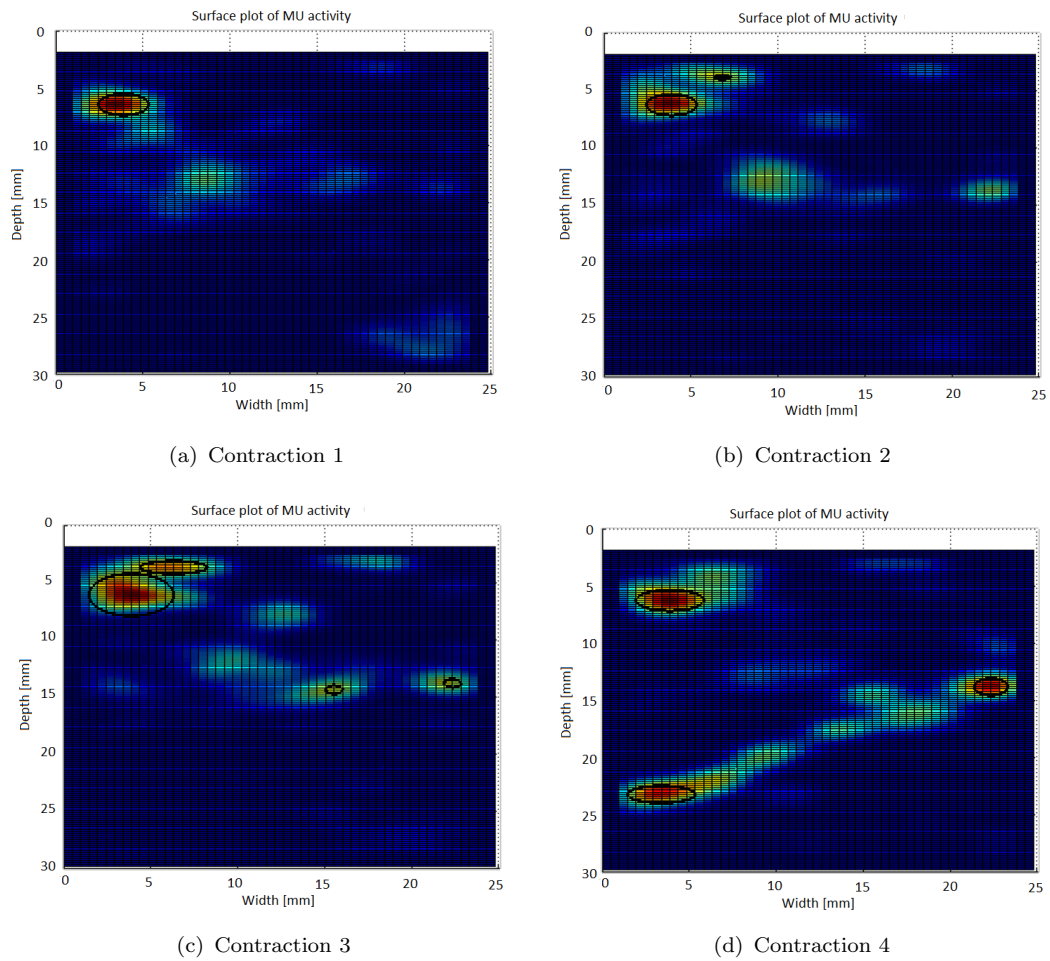


FIGURE 4.15: Strain rate images of the four contractions in figure 4.14

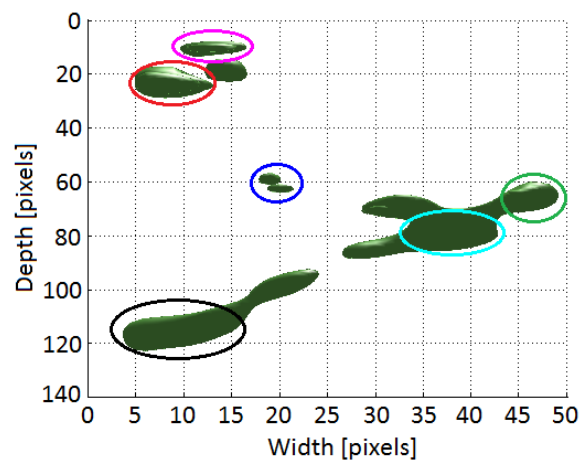


FIGURE 4.16: Isosurface plot of strain rate data with chosen regions of contraction marked

Most the chosen regions marked in 4.16 are present in all the three leading PCs shown in Figure 4.17. As a result, there are no "Motor units" in Figure 4.18(b) that expands in only one PC direction. The two Figures in 4.18 overlaps almost completely, which means that the chosen regions in Figure 4.16 covers most of the active MUs in the ultrasound sequence.

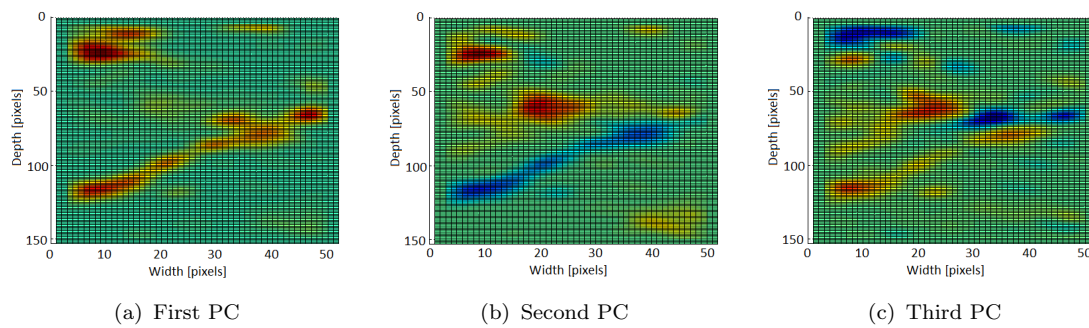
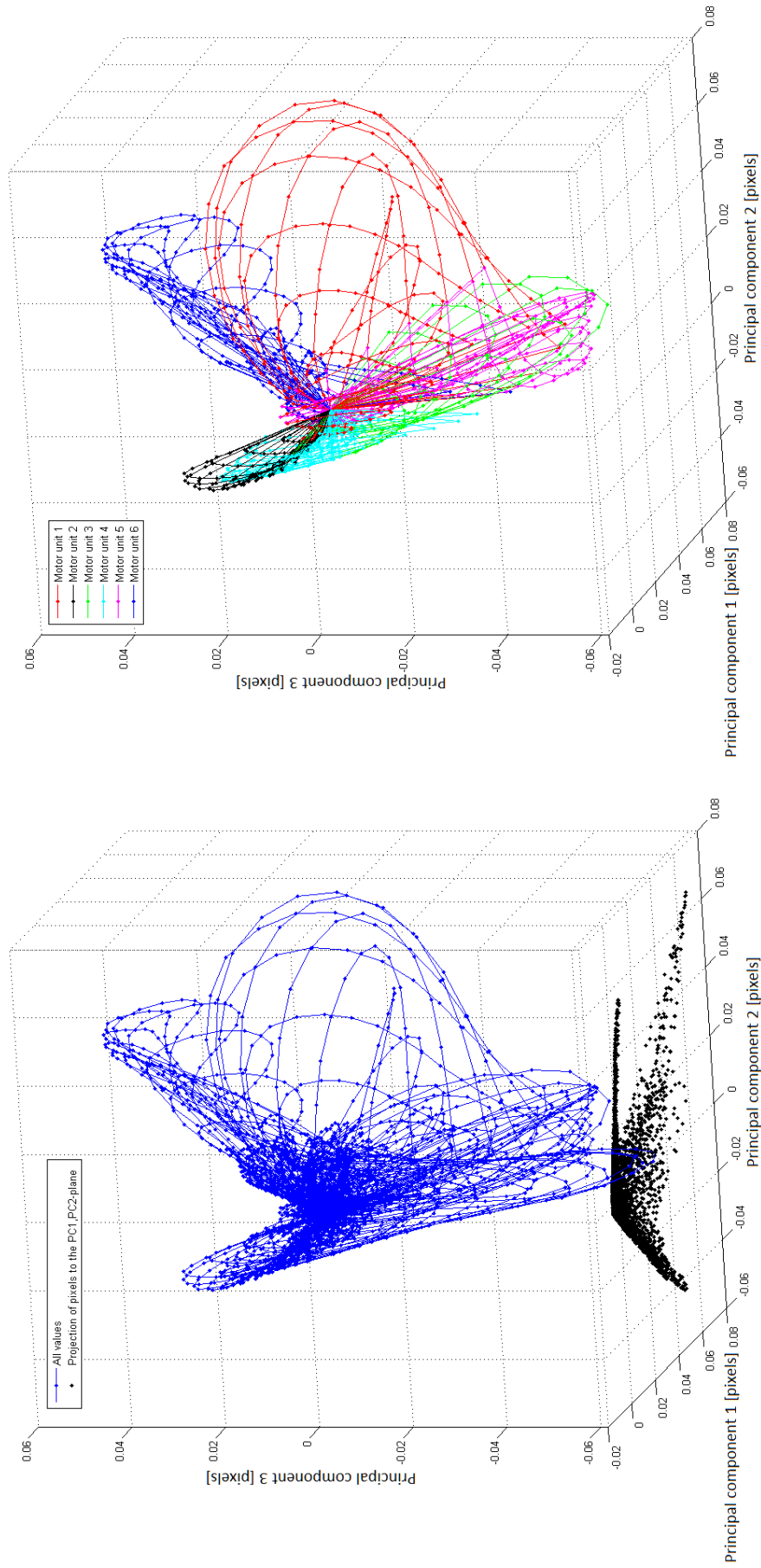


FIGURE 4.17: Strain rate images of the three leading principal components

If the two figures in 4.18 are compared with Figure 4.19, the one showing amount of activity per frame, it is seen that "Motor unit 1" through "Motor unit 5" expands in the same direction as "Contraction 4". This means that these five MUs are active during "Contraction 4", which is also shown in figure 4.15(d). The red region in Figure 4.18(b) represents "Motor unit 1". This "Motor unit" expands in a region which covers all the contractions in Figure 4.19, which is also seen in Figure 4.15, where all the contractions in Figure 4.19 expands up two the right at first, a region covered by both "Motor unit 1" and "Motor unit 6". "Contraction 1" and "Contraction 2" extends further from the origin. This means that "Motor unit 6" is less active during "Contraction 3" and "Contraction 4", which is also seen when looking at projections of the integrated SR images in Figure 4.15



(a) All pixel values

(b) Motor units in different colours

FIGURE 4.18: Feature extracting using SVD, pixels

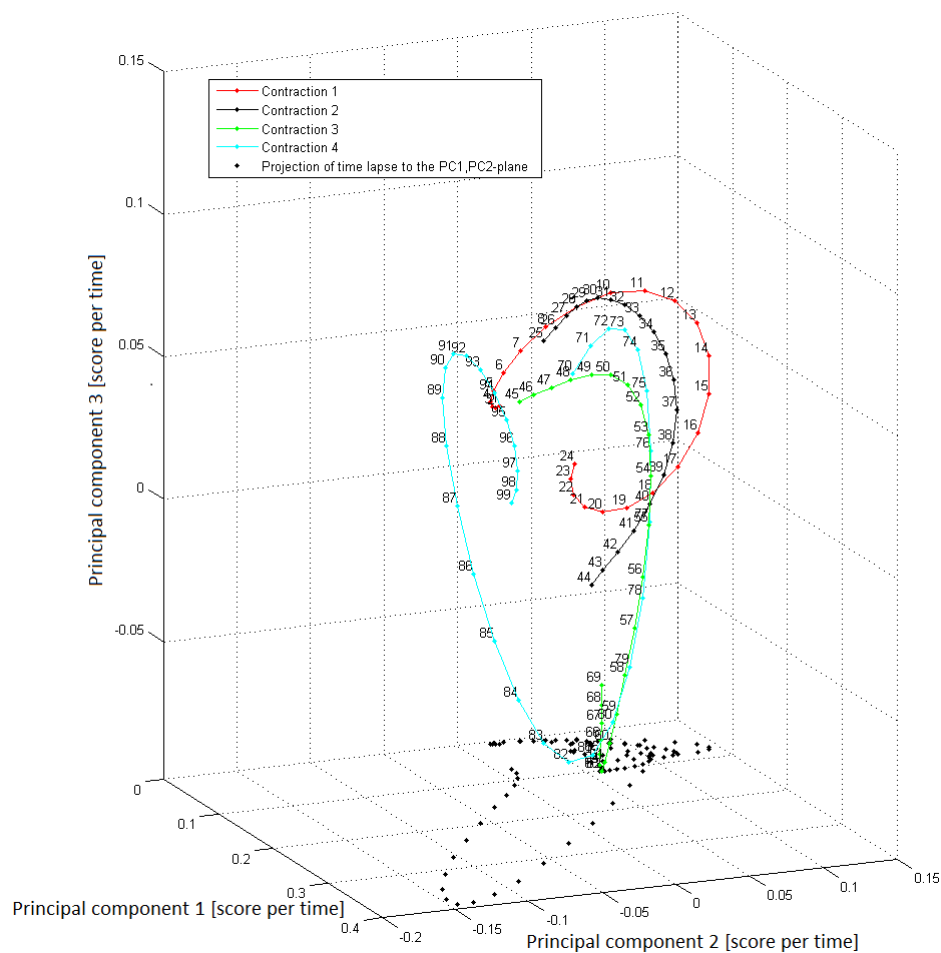


FIGURE 4.19: Feature extracting using SVD, showing score per time

As stated in Chapter 2.1.1, MUs are innervated asynchronously, which means that the visible MUs in each of the SR images in Figure 4.15 will not expand at the same time. This may happen, as the time between each frame is between 4.5ms and 8ms, depending on the FR, but this does not seem to be a problem in this sequence. By comparing Figure 4.18(b) and 4.19, it is possible to see the sequential activation of the MUs during each contraction. To show that the following interpretation of the data is satisfactory, four figures are shown in Appendix B, containing SR images during each contraction. If the numbers for each point in Figure 4.19 are followed sequentially, it is possible to pick out the same sequence of MU activation. Below is a list containing the sequential activation of individual MUs when comparing Figure 4.18(b) and 4.19.

- 
- "Contraction 1": "Motor unit 6" is followed by "Motor unit 1"
  - "Contraction 2": "Motor unit 6" is followed by "Motor unit 1" and some activity from "Motor unit 3" and "Motor unit 5"
  - "Contraction 3": "Motor unit 1" is followed by "Motor unit 3" and "Motor unit 5"
  - "Contraction 4": "Motor unit 6" is followed by "Motor unit 1", "Motor unit 3", "Motor unit 5", "Motor unit 3", "Motor unit 4" and "Motor unit 2".

This corresponds to the Figures in Appendix B.



# Chapter 5

## Discussion

### 5.1 Time delay between EMG and ultrasound response

By looking at the time difference between EMG and ultrasound response in the data from M. Heger (2013) [8] (example Figure 5.1), a time delay between 6.68ms and 15.38ms seems reasonable, which supports the claim that MU activity is captured in the ultrasound sequences. It is difficult to see the exact time delay in Figure 5.1 because of noise, but it is seen that the ultrasound response comes after the EMG response, but not by a greater delay than 15ms, which is marked with vertical red lines in Figure 5.1.

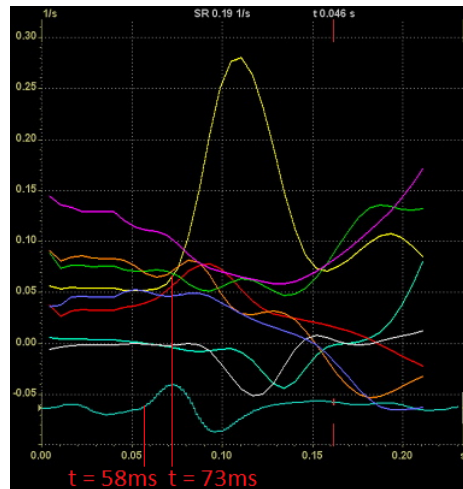


FIGURE 5.1: Figure showing an example of the Q-analysis window marked with a time delay of approximately 15 ms

## 5.2 Motor Unit Localization

The results from Chapter 4.3 and 4.4 shows that it is possible to locate individual MUs in a sequence of ultrasound SR images. The "Localization\_auto" algorithm, which locates MUs based on MU behaviour, manages to capture the MUs, but have problems locating overlapping MUs and smaller MUs. Even though this algorithm is not suitable to detect all the individual MUs present in a SR sequence, it might be a feasible algorithm for prosthetic use to increase the number DoFs. It manages to locate multiple MUs in ultrasound SR sequences containing one or multiple contractions, which can be used to classify different prosthetic actions. This algorithm has to be improved before it can be used in a real-time system, since the data processing is time consuming, but it might be feasible.

The projections of integrates SR images helped picking out the regions of contraction and contributed to show that the "feature extraction with SVD"-method is a potential method for spatial and temporal MU localization. In this study, the "feature extraction with SVD"-method is only a proposed method for MU localization and not an elaborated program. The results shows how this method can be used for localization of individual MUs in sequences containing single or multiple contractions. The analysis done in Chapter 4 indicates that this method



is a more robust and time-saving method for real-time systems, but calculation of SR and filtering is still needed for this method to work properly. In the examples in Chapter 4.4, only three PCs have been used to visualize the principal of this technique, but when automatised, more PCs can be used to localize all present MUs.

There have not been made any programs for automatic classification in this study, but a couple of data reduction and classification techniques have been proposed in Chapter 2.5. By looking at the Figures in 4.18, each MU is clustered together, where connecting pixels in the image is connected to each other. An algorithm for automatically finding clusters, like the proposed CA method in Chapter 2.5, could be used to classify each of these clusters (MUs).

A MATLAB tool-box, called multivariate image analysis (MIA), proposed by Harald Martens, is a possible tool for analysis of the kind of data shown in Figure 4.18. This tool-box provides a graphical interface and makes it easier to analyse multivariate images. It contains higher-level command-lines for performing PCA and different kinds of classification tools, like K-Means clustering, which can be useful for classification of MUs [23]. This package also makes it possible to automatically converting each point in Figure 4.18 to pixel position in SR images for better interpretation of the data.



# Chapter 6

## Conclusion

**The time delay between the ECG electrodes and ultrasound response** had an expected value of 2.38ms, which is small compared to the delay caused by the propagation velocity of a MUAP, which is between 4ms and 13ms. Because of this, the time delay between the ECG electrodes and the ultrasound scanner is almost negligible. An expected total time delay consisting of velocity propagation of biological signals and mechanical time delay was calculated to be between 6.68ms and 15.38ms.

**Motor unit localization** is possible by processing scans of isometric contractions from a state of the art ultrasound scanner in MATLAB. Ultrasound SR sequences can be used to locate MUs by picking out regions containing typical MU behaviour, but struggles to identify overlapping MUs as individual.

The "feature extraction using SVD"-method can be used for MU localization and quantification and is believed to have better prospects for future use, as it is able to localize all individual MUs present in an ultrasound SR sequence during one or multiple isometric contraction. No program for automatic localization of MUs were made for this method, but it may be accomplished by using this method in combination with a cluster based classification algorithm. The MIA tool-box in MATLAB is believed to ease the process of automatic localization.



# Chapter 7

## Future work

### 7.1 Data acquisition

This study indicates that the "feature extraction using SVD"-method could be used for classification of MUs. It has been tested on several raw-data from the ultrasound scanner, but more testing should be done to verify this method. To know that this method works satisfactory, new data should be collected and tested with the proposed method for feature extraction using SVD.

### 7.2 Automatic localization

The first step for further development would be to implement an automatic localization program by using the "feature extraction using SVD"-method presented in Chapter 2.6 in combination with a cluster based classification method. The MIA tool-box in MATLAB has build-in functions for image-enhanced cluster analysis and makes it possible to automatically display the results in image format. It also has importing and building functions to ease the work of assembling multivariate images.

### **7.3 Mapping of motor units**

If a satisfactory program for localization of individual MUs has been made, it would be interesting to see if it could be used to map individual MUs activity for typical human movements. This study only analyses data from small isometric contractions, so new experiments should be executed, where movements are carried out with a greater impact on the joints. If the proposed method manages to locate individual MU activity in ultrasound scans of muscle activity during normal movements, a map of which MUs that are active during different movements can be made. This could have a positive impact on the field of ergonomics, movement science, prosthetics and be of use to diagnose and treat muscle deficiencies.

### **7.4 Prosthetics**

If it is possible to map human motion by MU activity with the use of ultrasound, it could be a potential method for prosthetic control. The localization algorithm have to be optimized to work in real-time and ultrasound transducers has to be placed around the residual limb for this system to be functional as a method for prosthetic control, but it is believed that an ultrasound controlled prosthesis would increase the number of DoFs and be a more robust method for control compared to existing methods.

# Appendix A

## Project description

NTNU, Norwegian University of Science and Technology

Faculty of Information Technology, Mathematics and Electrical Engineering

Department of Engineering Cybernetics

Project Assignment

**Student name:** Max Heger

**Course:** TTK4900, Engineering Cybernetics, Master thesis

**Tittel (norsk):** Ultralydbasert Lokalisering og Kvantifisering av Kontraksjon i Skjelettmuskler

**Title (English):** Ultrasound Based Localization and Quantification of Skeletal Muscle Contraction

**Description:**

The skeletal muscles makes humans able to move, communicate and interact with the environment. Knowledge about muscle functionality in healthy as well as people with different disabilities are of great importance when it comes to both diagnostics and treatment. Detailed measurements of muscle function is very

important for control of electrical arm prostheses and other technological health care instruments.

Earlier experiments have demonstrated that modern ultrasound imaging makes it possible to show, localize and partly quantize geometrical changes caused by small isometric contractions in skeletal muscles on the scale of motor units. This assignment will pursue the results received from previous work by examine to what degree different motor units contributions can be localized and quantified when overlapping in time and space. This type of decomposition can be important for future technological health care instruments in the fields of ergonomy, movement science and rehabilitation technology.

1. Supplement earlier experiments with new measurements to confirm size and variation of the time difference between EMG and ultrasound images. Show to what degree the significance of this time delay have for the interpretation of earlier results.
2. Make an overview of relevant computer reduction methods and show how they have the potential of being used to decompose ultrasound data to localize and quantify signal contribution from individual motor units. Relevant methods can be basic techniques like Principal Component Analysis(PCA) alone or in combination with more advanced methods for image segmentation and classification.
3. Implement chosen methods on a suitable computer platform.
4. Identify optimal parameters for the ultrasound equipment, gather data and evaluate the methods.

This assignment also includes participation in a conference article based on this and the earlier assignment.

**Assignment received:** 14.01.2014

**Assignment delivered:** 05.06.2014



**Supervisors:**

Associate Professor Øyvind Stavdahl, Institutt for teknisk kybernetikk, NTNU

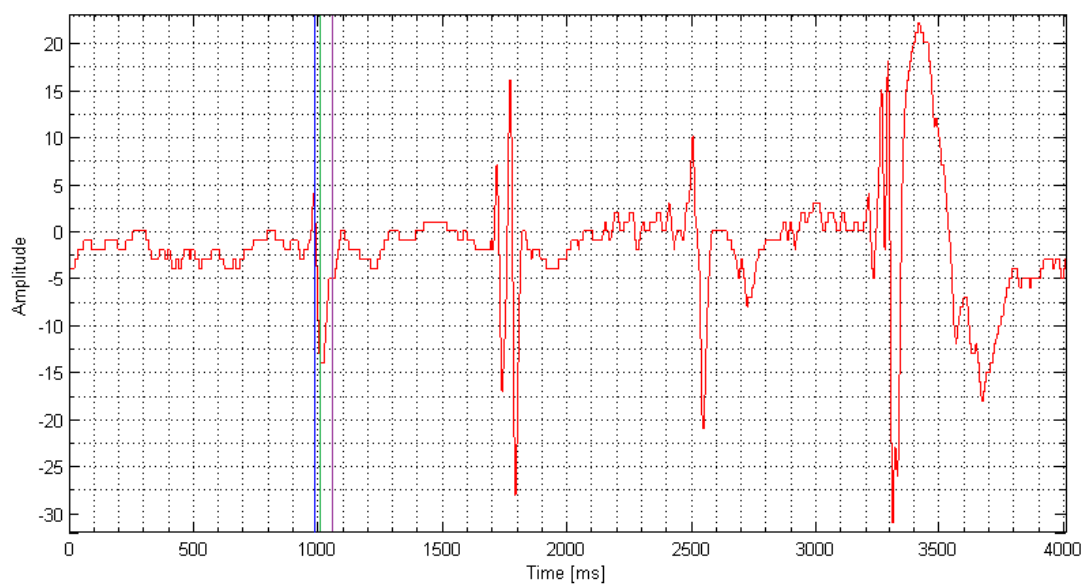
Professor Hans Torp, Institutt for sirkulasjon og bildediagnostikk, NTNU

Trondheim, June 2014

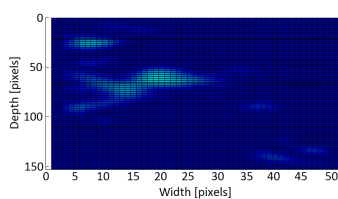


# Appendix B

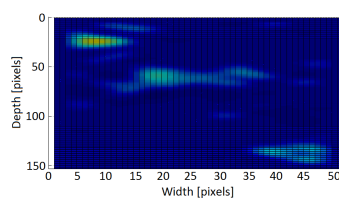
## Sequences of strain rate images



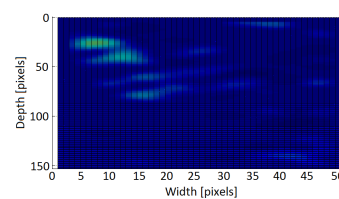
(a) EMG data for contraction 1



(b) Time step 1 (blue)

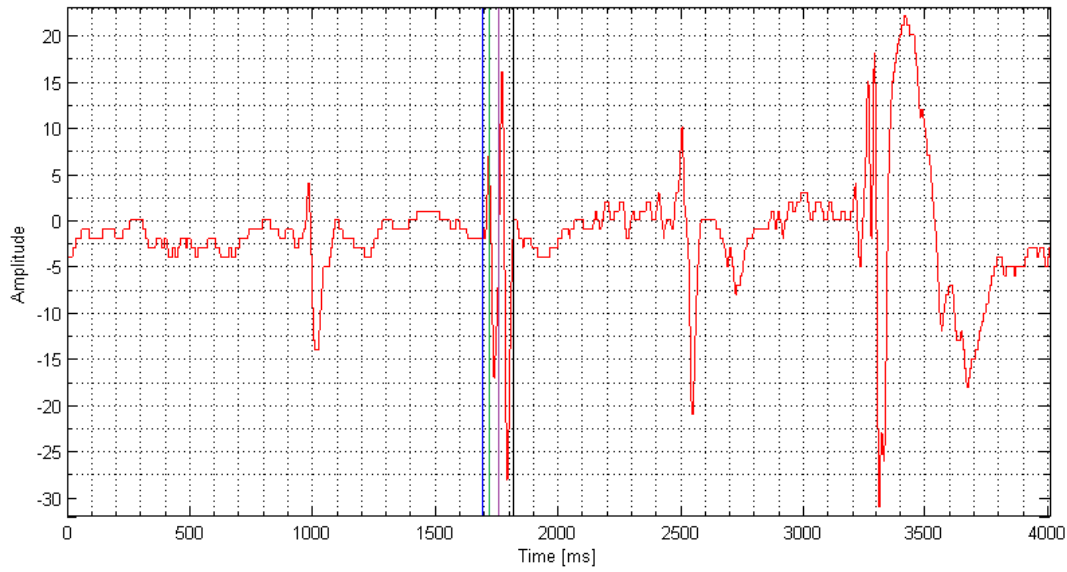


(c) Time step 2 (green)

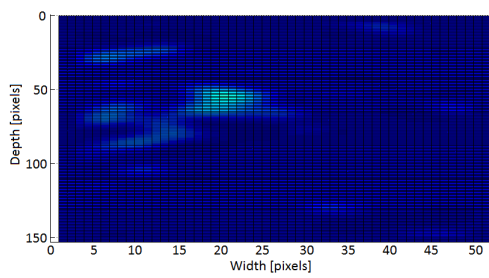


(d) Time step 3 (purple)

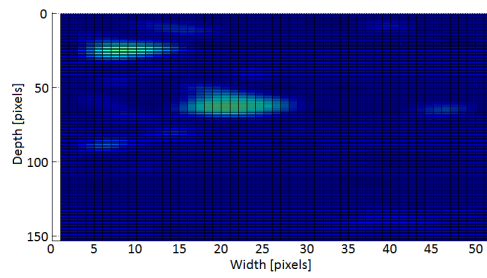
FIGURE B.1: EMG and SR data showing different frames during contraction 1



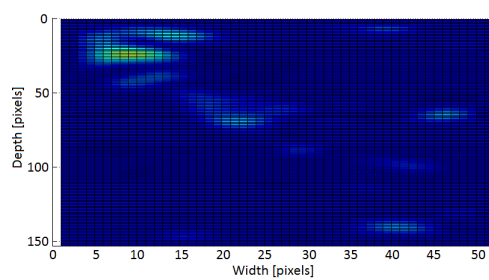
(a) EMG data for contraction 2



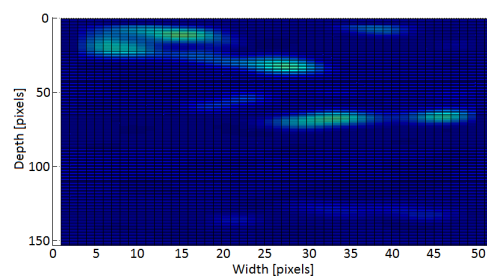
(b) Time step 1 (blue)



(c) Time step 2 (green)

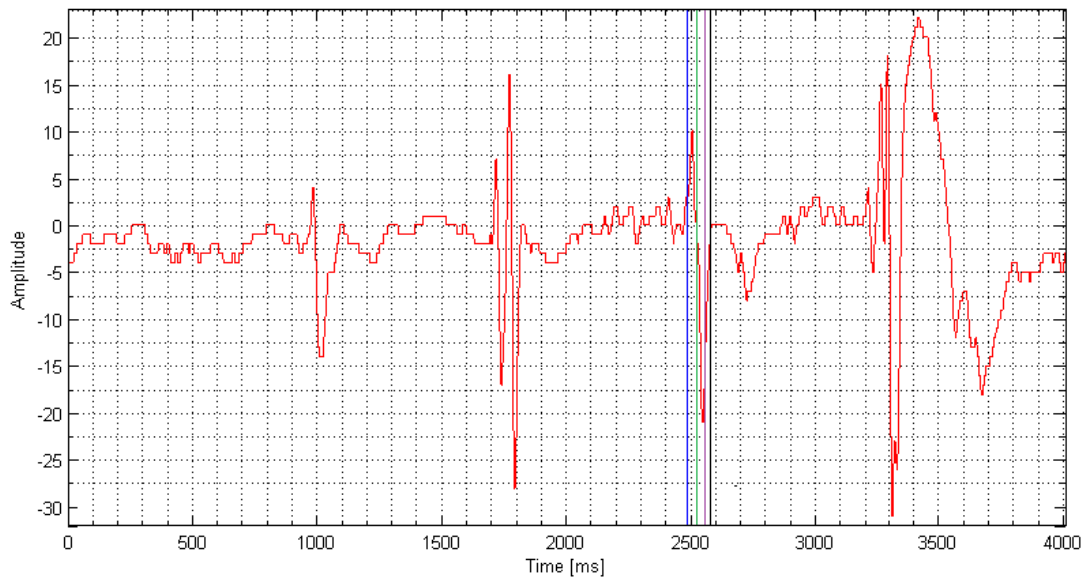


(d) Time step 3 (purple)

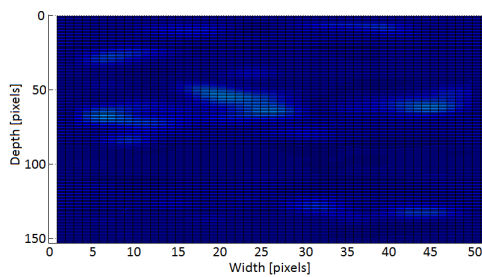


(e) Time step 4 (black)

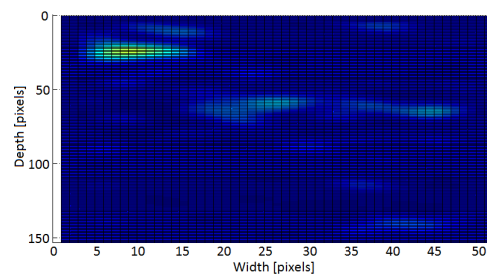
FIGURE B.2: EMG and SR data showing different frames during contraction 2



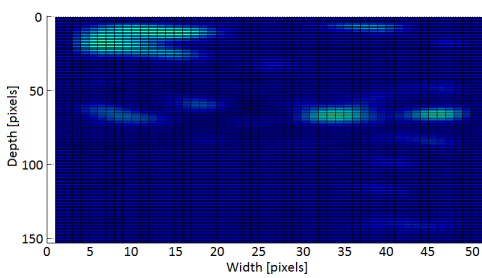
(a) EMG data for contraction 3



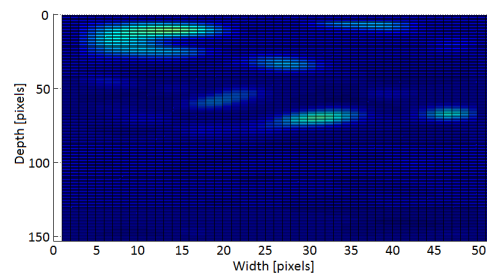
(b) Time step 1 (blue)



(c) Time step 2 (green)

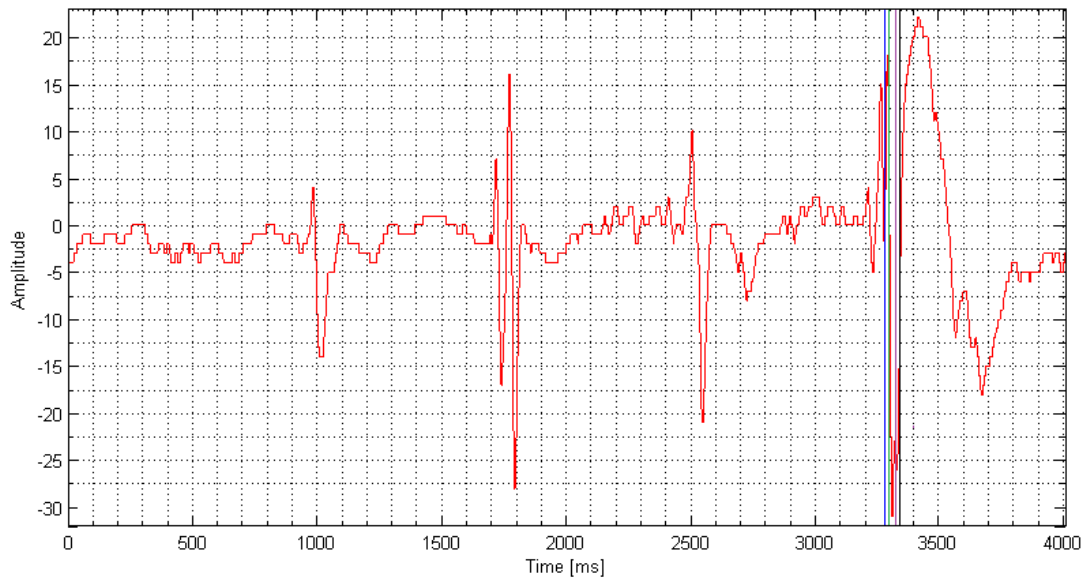


(d) Time step 3 (purple)

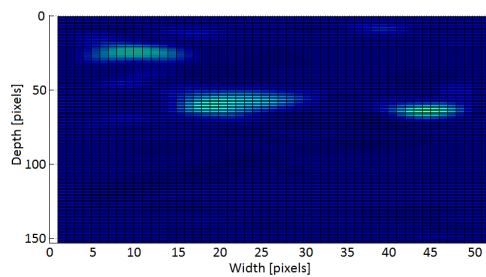


(e) Time step 4 (black)

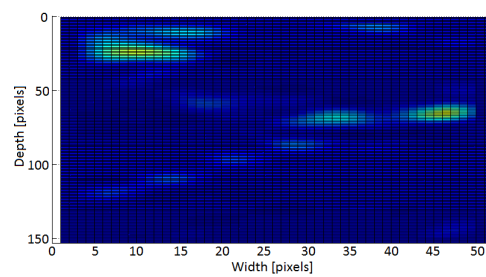
FIGURE B.3: EMG and SR data showing different frames during contraction 3



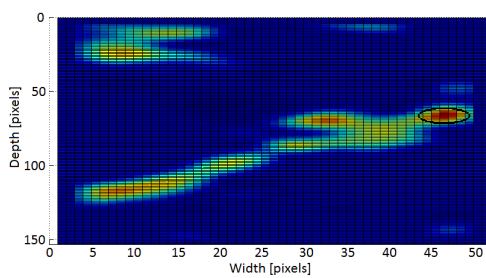
(a) EMG data for contraction 4



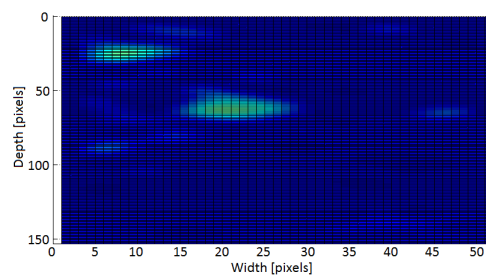
(b) Time step 1 (blue)



(c) Time step 2 (green)



(d) Time step 3 (purple)



(e) Time step 4 (black)

FIGURE B.4: EMG and SR data showing different frames during contraction 4

# Appendix C

## Abstract for IEEE article

### C.1 Ultrasound Strain Rate Imaging of Individual Muscle Motor Units

Max Heger, Øyvind Stavdahl & Hans Torp 1. April, 2014

Skeletal muscle is organized in motor units, each comprising a motor neuron and all its connected muscle fibres. The arrival of an action potential (a neural “impulse”) causes the fibers to contract – they exhibit a twitch. This study aimed for the spatiotemporal detection of individual twitches, which may allow for a more explicit study of muscle physiology and more dexterous prosthesis control.

We used a GE-Vingmed Vivid E9 ultrasound scanner and an ML6-15 linear probe in a clamped and fixed position over the biceps, giving images perpendicular to muscle fibers. The scans were executed by using “Strain rate”-mode in the test option “msc TVI” with a frequency of 15MHz, which results in a frame rate between 120 and 220 FPS, depending on depth. Recordings of tiny voluntary isometric muscle contractions were made, with ECG electrodes placed on each side of the probe to detect the associated motor unit action potentials (MUAPs).

The recordings were analyzed using the scanners quantitative analysis (Q-analysis) tool for measuring strain rates inside elliptical regions of interest (ROIs). Figure

1 shows an image containing eight ROIs. The figure includes b-mode images with and without strain rate measurements, respectively, and a graph showing the mean strain rate of the ROIs marked in the strain rate image. The turquoise graph at the lower right shows a single MUAP recorded simultaneously with the ultrasound data. The yellow strain rate graph shows what is believed to be the mechanical contraction associated with this single MUAP. The time delay from MUAP onset to twitch onset (approx. 8.75ms) and the spatial extent of the contracting region supports this claim. To our best knowledge, this is the first ultrasound image of a single motor unit twitch.

The results show that it is possible to image the mechanical response of a contracting muscle caused by a single motor unit by using ultrasonic strain rate imaging. This technique could thus be a future supplement to electromyography in certain applications.

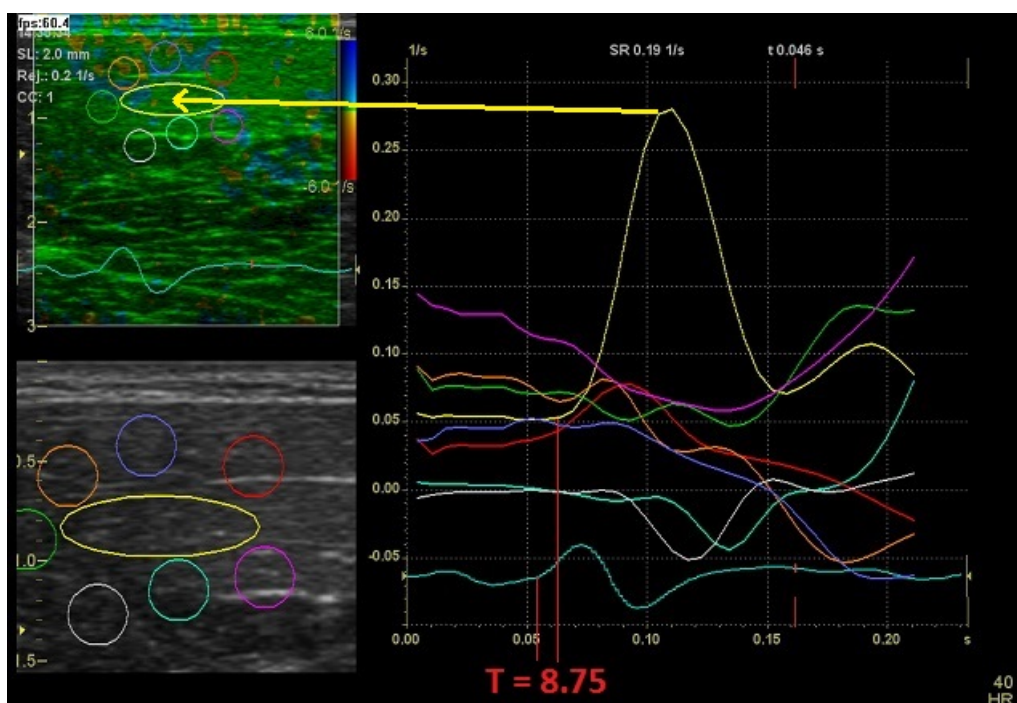


FIGURE C.1: Image of the Q-analysis tool showing one contraction



# Appendix D

## DVD overview

The DVD contains three main folders:

- Data
- MATLAB
- Report

The MATLAB folder contains five programs:

- ECG\_US\_TD: Program for calculating time delay between the ECG electrodes and ultrasound response.
- localization\_MU\_behaviour: Program for localization of individual MUs based on MU behaviour.
- mUDTDist: Program for loading ultrasound raw-data in MATLAB.
- SVD\_feature\_extraction: Program for feature extraction using SVD.
- SVD\_feature\_extraction\_ex: Program for the example for feature extracting using SVD in Chapter 2.6.

In the "Report files" folder, all the files for the report are found.

The "Data" folder contains two folders, one containing the data used to calculate the time delay between ECG electrode and ultrasound response and one containing the data for localization of MUs. Each folder in the "localization\_raw\_data" contains raw-data, saved information about centers, radii, arrival time of contractions and saved SR and EMG sequences.

# Appendix E

## Figure references

- Figure 2.1(a). Skeletal muscle anatomy: <http://training.seer.cancer.gov/anatomy/muscular/structure.html>
- Figure 2.1(b). Muscle fiber anatomy: [http://droualb.faculty.mjc.edu/Course%20Materials/Elementary%20Anatomy%20and%20Physiology%2050/Lecture%20outlines/skeletal\\_muscle\\_physiology.htm](http://droualb.faculty.mjc.edu/Course%20Materials/Elementary%20Anatomy%20and%20Physiology%2050/Lecture%20outlines/skeletal_muscle_physiology.htm)
- Figure 2.1(c). Cross section of upper arm: [http://www.dartmouth.edu/~humananatomy/figures/chapter\\_9/9-1.HTM](http://www.dartmouth.edu/~humananatomy/figures/chapter_9/9-1.HTM)
- Figure 2.2. Motor unit territory: From Javier Rodriguez-Falces et al. [20]
- Figure 2.3. MUAP propagation: <http://storm.uni-mb.si/semg/>
- Figure 2.5. Front end transmitting and receiving side:  
<http://www.maximintegrated.com/app-notes/index.mvp/id/4038>
- Figure 2.6. B-mode image of the anterior compartment of the upper arm:  
Got from M. Heger (2013) [8].
- Figure 2.7. Illustration of the Doppler effect:  
[http://www.school-for-champions.com/science/waves\\_doppler\\_effect.htm#.U2kmLvmSyPY](http://www.school-for-champions.com/science/waves_doppler_effect.htm#.U2kmLvmSyPY)

- Figure 2.8. Illustration of phase shift: <http://folk.ntnu.no/stoylen/strainrate/mathematics/index.html#Doppler>
- Figure 2.10. Cluster analysis: <http://www.pentalibra.com/content/cluster-analysis>
- Figure 2.14. Illustration of the SVM algorithm: [http://docs.opencv.org/doc/tutorials/ml/introduction\\_to\\_svm/introduction\\_to\\_svm.html](http://docs.opencv.org/doc/tutorials/ml/introduction_to_svm/introduction_to_svm.html)

# Bibliography

- [1] BAKER, KIRK. 2013. Single Value Decomposition Tutorial. Jan.
- [2] BAUN, JIM. 2004. *Principles of General and Vascular Sonography*.
- [3] BOHLING, GEOFF. 2006. Dimension Reduction and Cluster Analysis. March.
- [4] DAHL, TROND-OLAV. 2007 (June). *Velocity Estimation in Muscular Tissue by Ultrasound*.
- [5] DARIO FARINA, FRANCESCO NEGRO, MARCO GAZZONI ROGER M. ENOKA. 2008. Detecting the Unique Representation of Motor-Unit Action Potentials in the Surface Electromyogram. *Neurophysiol 100*, page 1223-1233.
- [6] DIANA D. SUHR, PH.D. Principal Component Analysis vs. Exploratory Factor Analysis.
- [7] GERALD E. LOEB, CLAUDE GHEZ. 2012 (March). *The Motor Unit and Muscle Action*. <http://pdf-release.net/2059755/The-Motor-Unit-and-Muscle-Action>.
- [8] HEGER, MAX. 2013 (Dec). *High-Definition Ultrasound Imaging of Contraction in Skeletal Muscles*.
- [9] IHLER, ALEXAANDER. 2012 (Nov). *PCA, SVD*. <https://www.youtube.com/watch?v=F-nfsSq42ow>.

- 
- [10] JING-YI GUO, YONG-PING ZHENG, QING-HUA HUANG XIN CHEN JUN-FENG HE HELEN LAI-WA CHAN. 2009. Performances of one-dimensional sonomyography and surface electromyography in tracking guided patterns of wrist extension. *Ultrasound in Med. & Biol.*, Vol 35, p.894-p.902.
- [11] JURE LESKOVEC, ANAND RAJARAMAN, JEFFREY D. ULLMAN. 2014. *Mining of Massive Datasets, Chapter 11: Dimensionality Reduction*. Fifth edn. Cambridge.
- [12] KIPPIN, TODD. 2013 (Aug). *Auditory and Somatosensory Systems*.
- [13] KIRKHORN, JOHAN. 1999. Introduction to IQ-demodulation of RF-data. September.
- [14] KOZMA, LASZLO. 2008 (Feb). *k-Nearest Neighbours algorithm (kNN)*. <http://www.lkozma.net/knn2.pdf>.
- [15] LEVI J. HARGROVE, GUANGLIN LI, KEVING B. ENGLEHART BERNARD S. HUDGINS. 2009. Principal Components Analysis Preprocessing for Improved Classification Accuracies in Pattern-Recognition-Based Myoelectric Control. *IEEE Transactions on Biomedical Engineering*, Vol. 56, No. 5, May.
- [16] M. ZECCA, S. MICERA, M. C. CARROZZA P. DARIO. 2002. Control of Multifunctional Prosthetic Hands by Processing the Electromyographic Signal. *Critical Reviews in Biomedical Engineering*, 30, page 459-485.
- [17] MARKOWITZ, JOSHUA. *Probe Selection, Machine Controls, and Equipment*.
- [18] OPENCV. *Introduction to Support Vector Machines*. [http://docs.opencv.org/doc/tutorials/ml/introduction\\_to\\_svm/introduction\\_to\\_svm.html](http://docs.opencv.org/doc/tutorials/ml/introduction_to_svm/introduction_to_svm.html).
- [19] PAUL E. BARKHAUS, SANJEEV D. NANDEDKAR. 2013. EMG Evaluation of the Motor Unit - Electrophysiologic Biopsy. *Medscape*, Aug.
- [20] PILLEN, SIGRID. 2010. Skeletal Muscle Ultrasound.

- [21] P.W. HODGES, PHD, L.H.M. PENDEL MSC R.D. HERBERT PHD S.C. GANDEVIA DSC. 2003. Measurement of muscle contraction with ultrasound imaging. *Muscle & Nerve June 2003, p.682-p.692.*
- [22] RANJANA AGARWAL, A. R. RAO. *Data Reduction Techniques.*
- [23] RESEARCH, EIGENVECTOR. *MIA\_Toolbox.*
- [24] RUMMEL, R. J. 2002 (Nov). *Understanding Factor Analysis.* <https://www.hawaii.edu/powerkills/UFA.HTM>.
- [25] S. BALAKRISHNAMA, A. GANAPATHIRAJU. Linear Discriminant Analysis - A Brief Tutorial.
- [26] SIDDHARTA SIKDAR, HUZefa RANGWALA, EMILY B. EASTLAKE IRA A. HUNT ANDREW J. NELSON JAYANTH DEVANATHAN ANDREW SHING JOSEPH J. PANCRAZIO. 2014. Novel Method Predicting Dexterous Individual Finger Movements by Imaging Muscle Activity Using a Wearable Ultrasonic System. *IEEE Transactions on Neural Systems and Rehabilitation Engineering, Vol. 22, Jan.*
- [27] STATSOFT. *k-Nearest Neighbours.* <http://www.statsoft.com/textbook/k-nearest-neighbors>.
- [28] STØYLEN, ASBJØRN. 1999. *Strain rate imaging of the left ventricle by ultrasound.*
- [29] STØYLEN, ASBJØRN. 2013a (Aug). *The Doppler Effect.* <http://folk.ntnu.no/stoylen/strainrate/mathematics/index.html#Doppler>.
- [30] STØYLEN, ASBJØRN. 2013b (Aug). *Phase Analysis.* <http://folk.ntnu.no/stoylen/strainrate/mathematics/index.html#Phase>.
- [31] TIAN SIVA TIAN, RAND R. WILCOX, GARETH M. JAMES. Data Reduction in Classification: A Simulated Annealing Based Projection Method.
- [32] TIM WU, HARALD MARTENS, PETER HUNTER KUMAR MITHRARATNE. 2014. Emulating facial biomechanics using multivariate partial least squares

- surrogate models. *International Journal for Numerical Methods in Biomedical Engineering*, May.
- [33] TODD R. FARRELL, RICHARD F. WEIR. 2005. Surface Vs. Implanted EMG for Multifunctional Prosthesis Control: Pilot Results. *MEC '05 Intergrating Prosthetics and Medicine*.
- [34] XIN CHEN, YONG-PING ZHENG, JING-YI GUO JUN SHI. 2010. Sonomyography (SMG) control for powered prosthetic hand: a study with normal subjects. *Ultrasound in Med. & Biol.*, Vol 36, p.1076-p.1088.
- [35] Y.P. ZHENG, M.M.F. CHAN, J. SHI-X. CHEN Q.H. HUANG. 2005. Sonomyography: Monitoring morphological changes of forearm muscles in actions with the feasibility for the control of powered prosthesis. *Medical Engineering & Physics*, Vol. 28.